esa

ECOSPHERE

Wildfire-mediated vegetation change in boreal forests of Alberta, Canada

Diana Stralberg,[1,2,]† Xianli Wang,[1,3] Marc-André Parisien,[4] François-Nicolas Robinne,[1] Péter Sólymos,[2] C. Lisa Mahon,[5] Scott E. Nielsen,[1] and Erin M. Bayne[2]

[1]*Department of Renewable Resources, University of Alberta, 751 General Services Building, Edmonton, Alberta T6G 2H1 Canada*
[2]*Department of Biological Sciences, University of Alberta, CW 405, Biological Sciences Building, Edmonton, Alberta T6G 2E9 Canada*
[3]*Great Lakes Forestry Centre, Canadian Forest Service, Natural Resources Canada, 1219 Queen St E, Sault Ste Marie, Ontario P6A 2E6 Canada*
[4]*Northern Forestry Centre, Canadian Forest Service, Natural Resources Canada, 5320 122 Street, Edmonton, Alberta T6H 3S5 Canada*
[5]*Canadian Wildlife Service, Northern Region, Environment and Climate Change Canada, 91780 Alaska Highway, Whitehorse, Yukon, Y1A 5X7 Canada*

Citation: Stralberg, D., X. Wang, M.-A. Parisien, F.-N. Robinne, P. Sólymos, C. L. Mahon, S. E. Nielsen, and E. M. Bayne. 2018. Wildfire-mediated vegetation change in boreal forests of Alberta, Canada. Ecosphere 9(3):e02156. 10.1002/ecs2.2156

Abstract. Climate-induced vegetation change may be delayed in the absence of disturbance catalysts. However, increases in wildfire activity may accelerate these transitions in many areas, including the western boreal region of Canada. To better understand factors influencing decadal-scale changes in upland boreal forest vegetation, we developed a hybrid modeling approach that constrains projections of climate-driven vegetation change based on topo-edaphic conditions coupled with weather- and fuel-based simulations of future wildfires using Burn-P3, a spatial fire simulation model. We evaluated eighteen scenarios based on all possible combinations of three fuel assumptions (static, fire-mediated, and climate-driven), two fire-regime assumptions (constrained and unconstrained), and three global climate models. We simulated scenarios of fire-mediated change in forest composition over the next century, concluding that, even under conservative assumptions about future fire regimes, wildfire activity could hasten the conversion of approximately half of Alberta's upland mixedwood and conifer forest to more climatically suited deciduous woodland and grassland by 2100. When fire-regime parameter inputs (number of fire ignitions and duration of burning) were modified based on future fire weather projections, the simulated area burned was almost enough to facilitate a complete transition to climate-predicted vegetation types. However, when fire-regime parameters were held constant at their current values, the rate of increase in fire probability diminished, suggesting a negative feedback by which a short-term increase in less-flammable deciduous forest leads to a long-term reduction in area burned. Our spatially explicit simulations of fire-mediated vegetation change provide managers with scenarios that can be used to plan for a range of alternative landscape conditions.

Key words: boreal forest; Burn-P3; climate change; ecosites; landscape simulation; wildfire.

Received 29 January 2018; accepted 7 February 2018. Corresponding Editor: Franco Biondi.

† **E-mail:** diana.stralberg@ualberta.ca

Introduction

Global climate change is anticipated to exert biome-scale influences on future vegetation patterns (Hickler et al. 2012, Rehfeldt et al. 2012) and disturbance regimes (Seidl et al. 2017), with profound influences on terrestrial biota. In the western boreal region of North America, there is evidence that recent anthropogenic climate change has resulted in more frequent and extensive moisture deficits (Peng et al. 2011), leading in turn to more frequent and larger fires (Kasischke

and Turetsky 2006), declines in forest biomass (Ma et al. 2012, Luo and Chen 2013, Hogg et al. 2017), and increased tree mortality (Hogg et al. 2002, Michaelian et al. 2010, Peng et al. 2011).

Continued warming and increased drought frequency is predicted to result in a general drying of the forest that may lead to widespread conversion of vegetation types (Hogg and Hurdle 1995, Schneider et al. 2009, Mbogga et al. 2010). In mesic upland mixed conifer–deciduous forests, warmer temperatures and increased natural disturbance frequencies could encourage competitive shifts from conifer-dominated to deciduous-dominated stands (Soja et al. 2007, Johnstone et al. 2010). These major ecosystem changes, which amount to an eventual shift from the boreal forest biome to a prairie grassland biome (Rehfeldt et al. 2012), will be slowed by the inertia of current forest systems, and the time lags imposed by growth, dispersal, and successional dynamics (Meier et al. 2012, Svenning and Sandel 2013, Wu et al. 2015). In the absence of disturbance, current forest systems may persist for extended periods, as the requirements for mature conifer persistence are less restrictive than for seedling establishment in drought-prone regions (Hogg and Schwarz 1997).

In most parts of the western boreal forest, where wildfires are particularly large and frequent (Stocks et al. 2002), it is well acknowledged that wildfires may trigger vegetation change (Johnstone et al. 2010). Across the Canadian boreal forest region, projected future increases in maximum summer temperatures and associated decreases in soil moisture suggest that area burned could increase by as much as fivefold by the end of the 21st century (Flannigan et al. 2005, Balshi et al. 2009, Boulanger et al. 2014). Consequently, this expected increase in natural disturbance events (i.e., wildfire) will almost certainly accelerate ecosystem shifts, reducing the lag in vegetation responses to climate conditions (Stephens et al. 2013). It should also create a younger forest mosaic, a trend that will be exacerbated by continued timber harvest and other industrial development activities (Schneider et al. 2003, Cyr et al. 2009, Hauer et al. 2010). Ultimately, such changes in forest composition and age structure may be enough to limit populations of some species. Thus, it is critical to understand decadal-scale dynamics of vegetation succession and disturbance in response to climate and land-use change, which are inextricably linked to wildfire dynamics.

Wildfire potential is a function of climate, fuel (flammable vegetation), and ignitions (Parisien et al. 2011*a*). In the western boreal region, the climate is becoming more fire-conducive, with more extreme fire-weather days already occurring, as well as projected for the future (Tymstra et al. 2007, Wang et al. 2015), thereby extending the length of the fire season (Wotton and Flannigan 1993, Flannigan et al. 2009). This increases the potential for more numerous fire ignitions and longer-burning (thus larger) fires (Wang et al. 2017). Lightning-caused ignitions are already numerous and will likely increase with future weather conditions (Krawchuk et al. 2009, Wotton et al. 2010, Veraverbeke et al. 2017). Fuels, however, may decrease over the next century, as forests become younger (Héon et al. 2014) and more deciduous-dominated (Johnstone et al. 2010) and therefore less-flammable (Cumming 2001, Bernier et al. 2016), providing some degree of eventual fuel limitation (Terrier et al. 2012). The grassland systems that are projected to be most suited to southern boreal climate conditions by the end of the 21st century (Schneider et al. 2009, Mbogga et al. 2010) represent a decrease in flammable biomass relative to forests, although wildfires there may still burn rapidly and cover large areas.

In order to capture both the direct effect of climate and the facultative effect of wildfire on vegetation change, dynamic models are needed to address short-term (i.e., decadal scale) vegetation trajectories. Spatially explicit landscape simulation models are numerous and well developed for many regions and systems (see Keane et al. 2004 for a review), but they have limited potential to predict outside the range of initial conditions. Disturbance-mediated ecosystem shifts are therefore not well developed due to the large spatial extents required to encompass the magnitude of expected climate change (but see Boulanger et al. 2016*b*). Dynamic global vegetation models capture broad-scale ecosystem shifts but are coarse in resolution and lacking in spatial and thematic detail. Furthermore, their potential to project climate-change responses is similarly constrained by the range of baseline conditions used for parameterization (Williams and Abatzoglou 2016).

Given the challenges associated with strictly dynamic models, hybrid approaches may be best suited—or at least most practically implemented—for broad-scale ecological inference in a climate-change context (Cushman et al. 2006, Gustafson 2013, Williams and Abatzoglou 2016). We developed such a hybrid approach for northern Alberta, Canada, by simulating scenarios of future fire behavior as a catalyst for climate-driven vegetation change. We thereby incorporated critical ecosystem processes, as well as empirically derived relationships, over broad climatic gradients. To develop these fire-mediated scenarios, we simultaneously took advantage of a wealth of systematically surveyed vegetation ecosite data (Boutin et al. 2009) and recent methodological developments in the simulation of future fire weather (Wang et al. 2015, 2016) and duration (Wang et al. 2014, 2017). Our focus was on upland vegetation, due in part to the additional complexities associated with wetland hydrologic feedbacks (Waddington et al. 2015), and the additional lags expected in these systems (Camill and Clark 2000), especially where permafrost degradation results in additional organic matter deposition (Vitt et al. 2000).

Our overarching objective was to identify decadal-scale effects of climate change on upland boreal forest vegetation, considering (1) topo-edaphic constraints to vegetation change, that is, soil moisture/nutrient conditions; and (2) changes in wildfire activity (as measured by simulated burn probability at a 500-m pixel level). Using a scenario evaluation framework and three complementary global climate models (GCM), we addressed the following set of specific questions for northern Alberta:

1. How will burn probability change over the 21st century as fire weather, fire-regime parameters, and fuels (vegetation types) change?
2. How much of the variability in future burn probability can be attributed to fire weather (as represented by different GCMs) vs. fire-regime parameters vs. fuels?
3. What are the combined projected impacts of climate change and wildfire on upland vegetation composition under different fire weather and fire-regime scenarios?
4. How do fire-mediated scenarios of change in upland vegetation differ from direct climate-change projections?

To address these questions, we evaluated eighteen scenarios based on all possible combinations of three fuel assumptions (static, fire-mediated, and climate-driven), two fire-regime assumptions (constrained and unconstrained, in terms of (1) the number of fires and (2) the duration of each), and three GCMs. Although our understanding of potential future fire-regime characteristics such as fire size and frequency is increasing, studies have mainly focused on changes in weather and climate; how these elements will co-vary as a function of vegetation change and other factors is largely unknown. Our goal was to bracket the possible range of outcomes while also exploring the influence of different assumptions about the future.

Methods

Study area

Our study area was the boreal forest region within the province of Alberta, Canada, with a total area of 438,063 km^2, ranging from ~55° N to 60° N latitude at the border with the Northwest Territories (Fig. 1). Specifically, we focused our inference on Alberta's boreal natural regions (boreal forest and Canadian Shield), as well as the lower portion of the foothills natural region (Natural Regions Committee 2006).

Boreal Alberta is characterized by a strongly continental climate. The average annual moisture balance is slightly positive (Hogg 1994), and fire is the predominant natural disturbance. Geologically, the boreal region of Alberta primarily consists of the boreal plain, an area of deep marine sediments, and a small section of the Canadian Shield (eroded Precambrian rock) in the northeastern corner of the province. Upland forests are composed primarily of aspen (*Populus tremuloides*) and white spruce (*Picea glauca*) in various mixtures, with a tendency for the former to dominate on warmer, more exposed sites, and the latter on colder and more sheltered sites. Extensive forested wetlands are also found, where black spruce (*Picea mariana*) and eastern larch (*Larix laricina*) dominate on cold, poor wetland soils. Forests on the granitic expanse of the western Canadian Shield are composed mostly of black spruce and jack pine (*Pinus banksiana*). Foothills forests contain primarily lodgepole pine (*Pinus contorta*), white spruce, and aspen.

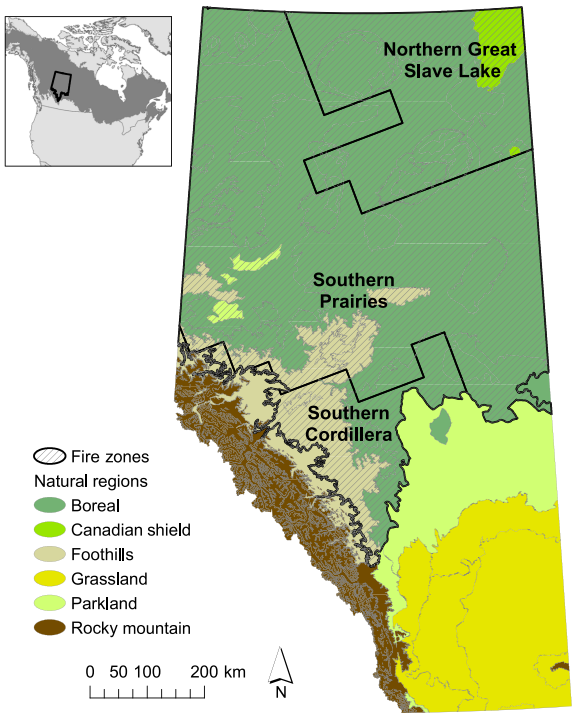

Fig. 1. Northern Alberta study area, natural regions, and fire zones (Boulanger et al. 2012) used for stratification of Burn-P3 fire simulations.

Alberta's wildfire regime is characterized by large, stand-renewing fires primarily initiated by lightning strikes, and a fairly long season, starting early April and ending late September (Tymstra et al. 2005). Most fire activity occurs in the boreal region, particularly in the northern part of the province, with less activity in the foothills region (Tymstra et al. 2005).

The region contains little urban/rural development (<2%), and agricultural activities are climate-limited, covering 10.6% of the boreal region and 3.0% of the foothills region (Schieck et al. 2014). In terms of total area, forestry and energy sector footprints are estimated to cover just 2.7% and 1.7%, respectively, of the boreal region (including the Canadian Shield portion), and 16.9% and 2.5%, respectively, of the foothills region (Schieck et al. 2014). However, the industrial land-use footprint is quite extensive, consisting of a combination of timber harvest blocks; oil, gas, and bitumen wells; mines; and a network of linear features that includes pipelines, seismic lines, powerlines, and variety of other roads and trails (Schneider et al. 2003). Fire activity is generally suppressed within the immediate vicinity of human disturbance, but may also be enhanced by the permeation of human infrastructure and activities in remote regions (Robinne et al. 2016).

Vegetation model and simulation overview

To assess potential future patterns of vegetation change and wildfire activity, we developed new 500-m resolution vegetation layers to use as fuel inputs to fire simulations under various scenarios. These were achieved by modeling vegetation as a function of geology, terrain, and climate in a two-stage process using a random forest (Breiman 2001) machine-learning algorithm, with performance assessed according to out-of-bag (OOB) classification accuracy (Appendix S1). Future potential vegetation distributions were projected as a function of future climates, assuming that current topo-edaphic characteristics (i.e., geology, topography, and resulting soil moisture and nutrient conditions) would remain constant over the 90-yr study period. We held wetlands constant and focused our analysis on upland forests, where vegetation transitions are more dynamic than in wetland systems (Schneider et al. 2016). Specifically, we first constructed models relating current ecosite type (defined as soil moisture and nutrient class) to geology, terrain, and climate. We then modeled vegetation as a function of ecosite type, terrain, and climate within our boreal study area, and projected future potential, hereafter "climate-driven," vegetation based on future climate variables, holding ecosite type and terrain variables constant (Fig. 2a). Climate variables were based on historical normals (1961–1990) and climate projections for three future time periods: 2011–2040, 2041–2070, and 2071–2100. Global climate models with available future fire weather projections (Wang et al. 2017) were from the Coupled Model Intercomparison Project, Phase 5 (CMIP5, Taylor et al. 2012): CanESM2 (Chylek et al. 2011), CESM1-CAM5 (Hurrell et al. 2013), and HadGEM2-ES (Jones et al. 2011). We used representative concentration pathway 8.5, to capture the conditions that are to be expected without dramatic reductions in greenhouse gas emissions or technological fixes (Fuss et al. 2014).

Assuming that vegetation can only reach its future projected climatic potential if catalyzed by wildfire or other disturbance (Schneider et al.

2009), we simulated several scenarios of fire-mediated vegetation change over the 21st century, based on simulated future daily fire weather and two different sets of future fire-regime assumptions (constrained and unconstrained, in terms of the number of fires and the duration of fire spread conditions; Table 1; Appendix S2: Table S1). Simulations were conducted using Burn-P3 (P3 = probability, prediction, and planning; Parisien et al. 2005), a spatially explicit fire model that simulates the ignition and growth of individual fires on the landscape using the Prometheus fire growth engine (Tymstra et al. 2010). The Prometheus model calculates fire growth based on fuels and terrain according to the Canadian Fire Behavior Prediction (FBP) System (Forestry Canada Fire Danger Group 1992) and fire spread mechanisms (Richards 1995). Burn-P3 uses Prometheus to simulate individual fires deterministically for one fire year, and this process is repeated for a large number of iterations using variable ignitions and weather. We used Burn-P3 outputs of simulated fires to update burned areas based on climate-projected potential future vegetation for three 30-yr periods from 2011 to 2100 (Fig. 2b). In order to evaluate the importance of future vegetation for burn probability, we also simulated fires for the same time periods with static and climate-driven fuel scenarios, where baseline and future climate-predicted vegetation, respectively, were used as inputs to Burn-P3 (Table 1; Appendix S2: Table S1).

Fire simulation—general parameters

Each Burn-P3 model iteration represents one realization of parameters for one year. Within this period, two seasons were defined to stratify the temporal variability in fire ignition and spread: spring (April 15–May 24) and summer (May 25–Sept 15). The start date of the spring season and the end date of the summer season correspond, on average, to the earliest and latest dates at which fires ≥200 ha occur. The start date of the summer season corresponds to green-up of broadleaf trees. The fire seasons were determined through summary explorations of weather and, in particular, of the distributions of fire numbers and area burned throughout the year. Percent grass curing (dry dead grass) was estimated to be 70% for the spring season and 55% for the summer season. For both seasons, we assumed spatially random ignitions within each fire zone and 4 h of potential fire growth per day.

Due to the large extent of our study area, and the variation in fire regimes it contains, we stratified it following the fire zone delineation of Boulanger et al. (2012). Three distinct fire zones were contained in our study area: the northern Great Slave Lake zone (highest fire frequency), the Southern Prairies zones (intermediate), and the Southern Cordillera zone (lower fire frequency; Fig. 1). To allow fires to begin outside the study area and thus avoid edge effects, we calculated a 30-km buffer around the study area. To inform topographic influences on fire spread, we used a 500-m digital elevation model corresponding with the resolution of our fuel inputs (Jarvis et al. 2008). As a sensible modeling shortcut, only fires ≥200 ha were modeled (Parisien et al. 2005); these large fires are responsible for approximately 97% of the total area burned in Canada (Stocks et al. 2002).

Fire simulation—fire weather parameters

A primary input to Burn-P3 is daily fire weather, which consists of daily noon observations of surface air temperature, relative humidity, 10-m open wind speed, and 24-h accumulated precipitation, as well as corresponding Fire Weather Index (FWI) System (Van Wagner 1987) variables, which are used to track daily fuel moisture conditions and potential fire behavior. Following the methods of Wang et al. (2014), two of the FWI System variables, the duff moisture code (DMC, a scaled measure of duff fuel layer moisture content) and the FWI (a scaled indicator of fire intensity; Van Wagner 1987), were used to determine fire duration, which in turn constrains the size of a fire. The DMC was used to determine the rain-free periods during which fires can burn, whereby a DMC <20 results in extinguishment (Anderson 2010). During those intervals, only days with FWI ≥ 19 were used to simulate fire growth, as suggested by Podur and Wotton (2011).

Historical daily fire weather data were obtained from an interpolated 3-km resolution grid provided by the Canadian Forest Service based on surface observations taken between April 1 and September 30 from 1981 to 2010 (Wang et al. 2015). Future fire weather data for

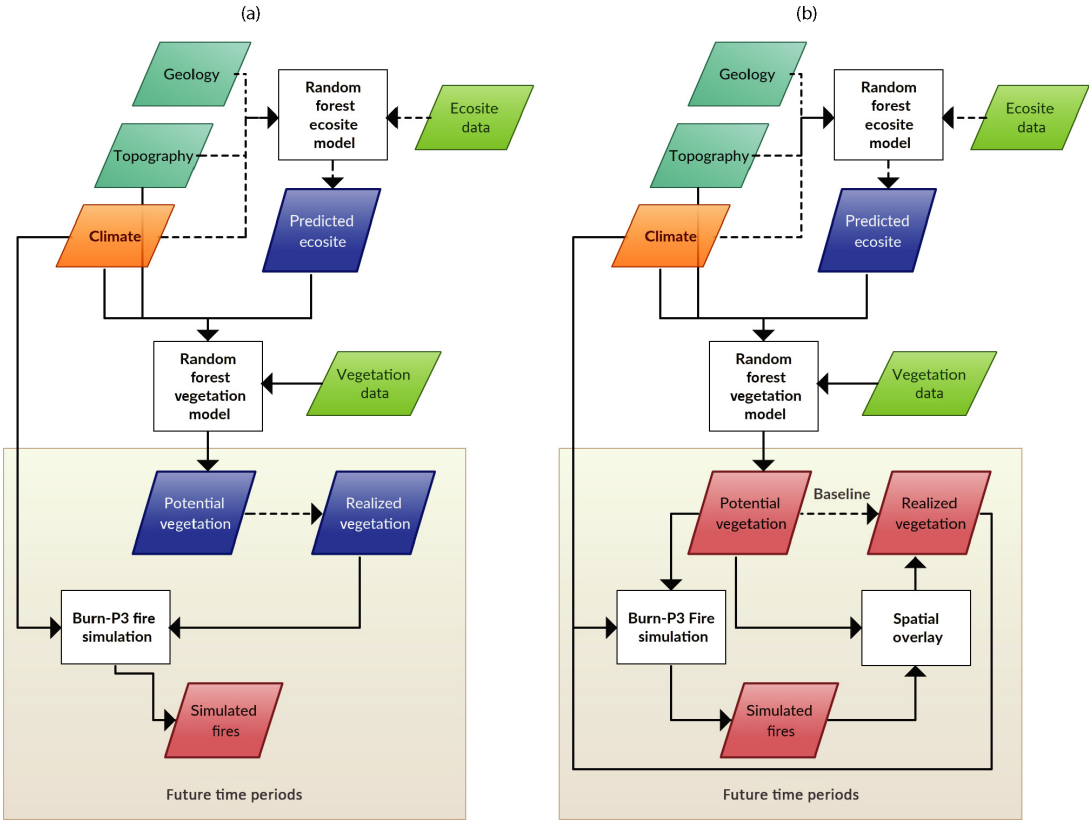

Fig. 2. Workflow diagram for (a) climate-driven and (b) fire-mediated scenarios. Green parallelograms represent point level data inputs; turquoise parallelograms are static raster data inputs; orange parallelograms are dynamic raster data inputs; blue parallelograms are static raster data outputs; red parallelograms are dynamic raster data outputs. White boxes are model processes. The elements outside the gray box represent the ecosite and vegetation modeling components; the elements within the gray box represent the iterative fire simulation and vegetation update components, which are repeated for three time periods: 2011–2040, 2041–2070, and 2071–2100.

all scenarios were from Wang et al. (2017), who applied monthly change anomalies to daily baseline values to translate future monthly climate projections from GCM simulations into future daily fire weather values for the periods 2011–2040, 2041–2070, and 2071–2100. One hundred and six points, separated by at least 40 km, were randomly sampled from the grid to represent daily fire weather conditions (i.e., pseudo-weather stations) for baseline and future time periods, stratified by fire zone.

Fire simulation—fire-regime parameters

For the unconstrained fire-regime scenarios, we assumed climate-related increases in fire-regime parameters—the number of escaped fires (Flannigan et al. 2006, Kasischke and Turetsky 2006) and the duration of fire spread conditions (Wang et al. 2017)—and estimated these parameters for future time periods based on daily fire weather projections. For the number of fires, we used linear regression analysis to relate the number of historical fires in a given ecoregion to monthly temperature (mean noon values) and precipitation values for the corresponding year. The resulting models (Appendix S2: Table S2) were applied to a sample of future weather values in order to generate future distributions of the number of escaped fires in each ecoregion. Resulting distributions were combined into a single distribution, according to

Table 1. Forest change scenarios evaluated (see Appendix S2: Table S1 for full specifications).

ID	Fuel scenario	Fire-regime scenario	GCM
1	Static fuels	Constrained	CanESM2
2	Static fuels	Constrained	CSIRO
3	Static fuels	Constrained	HadGEM2
4	Static fuels	Unconstrained	CanESM2
5	Static fuels	Unconstrained	CSIRO
6	Static fuels	Unconstrained	HadGEM2
7	Climate-driven fuels	Constrained	CanESM2
8	Climate-driven fuels	Constrained	CSIRO
9	Climate-driven fuels	Constrained	HadGEM2
10	Climate-driven fuels	Unconstrained	CanESM2
11	Climate-driven fuels	Unconstrained	CSIRO
12	Climate-driven fuels	Unconstrained	HadGEM2
13	Fire-mediated fuels	Constrained	CanESM2
14	Fire-mediated fuels	Constrained	CSIRO
15	Fire-mediated fuels	Constrained	HadGEM2
16	Fire-mediated fuels	Unconstrained	CanESM2
17	Fire-mediated fuels	Unconstrained	CSIRO
18	Fire-mediated fuels	Unconstrained	HadGEM2

Note: GCM, global climate model.

Burn-P3 input requirements, with the distribution across ecoregions stratified according to historical fire frequencies.

For fire duration, we estimated future spread-day distributions following the methods of Wang et al. (2014, 2017). We determined the FWI-based potential spread days in the baseline period and converted potential (i.e., weather-based) spread days to realized (i.e., actual) days of fire spread via a conversion factor obtained from simple linear regression (Wang et al. 2014). Future potential spread-day distributions were predicted from weather data and then used to estimate realized spread-day distributions using the conversion factor calculated for the baseline period, following Wang et al. (2017, see Appendix A). As part of the model calibration process, we truncated the baseline spread-day distribution so that the resulting fire-size distribution and number of fires best matched the observed distribution from historical data. Fires used for calibration were from the period 1980–2014 and were obtained from the Canadian National Fire Database (Canadian Forest Service 2015).

For the constrained fire-regime scenarios, we used future weather inputs, but held the number of escaped fires and spread-day distributions constant (Appendix S2: Table S1). To evaluate the relative contribution of the number of escaped fires vs. spread-day distributions, we ran an additional set of static-fuel scenarios holding each of these fixed at baseline conditions and manipulating the other factor (Appendix S2: Table S1).

Fire simulation—fuel parameters

Fuel inputs were directly derived from our vegetation model by converting vegetation types to fuel types as defined by the FBP System (Table 2), where each fuel type exhibits characteristic fire behavior depending on weather conditions and slope. For the 30-km buffer region, we used a mirrored representation of the input fuel grid. Fuel types can be broadly categorized as coniferous, deciduous, mixedwood, and grass. The coniferous fuel types are the most conducive to fire ignition and spread. The deciduous (D-1/2) and mixedwood (M-1/2) fuel types have a greater susceptibility to fire growth in the spring, before leaf flush, than later in the season. Fire spread potential in the grass (O-1) fuel type is also more flammable in the spring than in midsummer because most of its biomass consists of dead material with very low moisture content during this season.

For the baseline period (1981–2010) and for 2011–2040, we used modeled fuels corresponding with historical climate normals from 1961 to 1990, which reflect the historical growing conditions for Alberta forests better than do current climate conditions (see Appendix S1 for vegetation modeling details). For future time periods, three sets of fuel scenarios were considered (Table 1). For static-fuel scenarios, historical fuels were held constant. For climate-driven scenarios, fuels were based on climate-projected potential vegetation for three GCMs. For fire-mediated scenarios, fuel inputs to 2041–2070 fire simulations were derived by updating the historical fuel layer according to 2011–2040 fire simulations (Fig. 2b). Given the stochastic nature of Burn-P3, we randomly selected one model iteration to reflect each year in the 30-yr period. Fire polygon outputs from 30 randomly selected years were combined to represent the area burned within the baseline period. For these burned areas, we updated the fuel layer based on future projected vegetation for 2011–2040 climate conditions. Elsewhere, baseline fuels were retained. Together

Table 2. Ecosite and vegetation types considered.

Code	Ecosite	Vegetation description	FBP	Cover type	Upland	Forest
1	PX	Poor-Xeric Grassland	O-1	Grassland	1	0
2	PX	Poor-Xeric Jack Pine	C-1	Conifer	1	1
3	PM	Poor-Mesic Grassland	O-1	Grassland	1	0
4	PM	Poor-Mesic Pine	C-3	Conifer	1	1
5	PM	Poor-Mesic Black Spruce	C-2	Conifer	1	1
6	PG	Poor-Hygric Black Spruce	C-2	Conifer	0	1
7	PD	Poor-Hydric Black Spruce / Larch	C-1	Conifer	0	1
8	PD	Poor-Hydric Shrub	O-1	Shrub	0	0
9	MX	Medium-Xeric Grassland	O-1	Grassland	1	0
10	MX	Medium-Xeric Aspen Mix	M-1/2	Mixedwood	1	1
11	MX	Medium-Xeric Pine	C-1	Conifer	1	1
12	MX	Medium-Xeric Spruce	C-1	Conifer	1	1
13	MM	Medium-Mesic Grassland	O-1	Grassland	1	0
14	MM	Medium-Mesic Aspen	D-1/2	Deciduous	1	1
50	MM	Medium-Mesic Boreal Aspen	M-1/2	Mixedwood	1	1
15	MM	Medium-Mesic Aspen Mix	M-1/2	Mixedwood	1	1
16	MM	Medium-Mesic Pine	C-3	Conifer	1	1
17	MM	Medium-Mesic Pine Mix	C-3	Conifer	1	1
18	MM	Medium-Mesic White Spruce	C-2	Conifer	1	1
19	MG	Medium-Hygric Grassland	O-1	Grassland	0	0
20	MG	Medium-Hygric Poplar Mix	M-1/2	Deciduous	0	1
21	MG	Medium-Hygric Spruce Mix	C-2	Conifer	0	1
22	MG	Medium-Hygric Black Spruce Mix	C-2	Conifer	0	1
25	MD	Medium-Hydric Shrub Fen	O-1	Shrub	0	0
26	MD	Medium-Hydric Black Spruce Fen	O-1	Conifer	0	1
27	RM	Rich-Mesic Grassland	O-1	Grassland	1	0
28	RG	Rich-Hygric Shrubland	O-1	Shrub	0	0
29	RG	Rich-Hygric Poplar	D-1/2	Deciduous	0	1
30	RG	Rich-Hygric Lodgepole Pine	C-3	Conifer	0	1
31	RG	Rich-Hygric Spruce	C-2	Conifer	0	1
32	RD	Rich-Hydric Grass Fen	O-1	Grassland	0	0
33	RD	Rich-Hydric Shrub Fen	O-1	Shrub	0	0
34	RD	Rich-Hydric Black Spruce	O-1	Conifer	0	1
35	SD	Marsh	Nonfuel	Grassland	0	0
39*	OW	Open Water	Nonfuel	None	0	0
41*	AG	Agriculture	Nonfuel	None	0	0
42*	UR	Urban	Nonfuel	None	0	0
43*	NF	Other Nonfuel	Nonfuel	None	0	0

Notes: Codes with * were patched in post-hoc based on remotely sensed 2000 landcover (Pan et al. 2014). FBP, Canadian Forest Fire Behavior Prediction System fuel type for input to Burn-P3; O, grass fuel; D, deciduous fuel; M, boreal mixedwood fuel; C, conifer fuel.

with other Burn-P3 inputs, these fuel modifications were the inputs for a single model run. This process was repeated 10 times to capture the stochastic variability across Burn-P3 iterations, and for vegetation projections from three different GCMs (listed in previous section), for a total of 30 runs × 300 iterations = 9000 individual Burn-P3 iterations for the 2041–2070 time period. The same process was repeated for inputs to the 2071–2100 fire simulations, with fuels for areas burned in the 2041–2070 runs updated according to projected 2041–2070 vegetation. Simulated fires from the end-of-century runs were used to update fuels according to projected 2071–2100 vegetation in areas burned. This was repeated for both sets of fire-regime scenarios—constrained and unconstrained—resulting in a total of 151 runs and 129,000 iterations (see

breakdown in Appendix S2: Table S1). Our exploration of fire-regime parameters (relative influence of number of escaped fires vs. spread-day distributions) for static-fuel scenarios resulted in an additional 12 runs and 36,000 iterations (Appendix S2: Table S1).

Fire and forest change analysis

To assess changes in wildfire activity in the future relative to the baseline period (Objective 1), we evaluated projected changes in area burned at the 500-m pixel level by calculating burn probability: the proportion of individual Burn-P3 iterations for which a given pixel was burned within a given time period, and for a given scenario and GCM. For fire-mediated scenarios, we combined results from 300 iterations for each of 10 fuel iterations, resulting in a total of 3000 iterations. For static and climate-driven scenarios, we ran 3000 iterations for each time period (a number of iterations deemed sufficient to assess the spatial patterns and overall mean change in burn probability).

To assess the influence of different sources of variation on simulated burn probability (Objective 2), we sampled a 20-km regular grid of 900 points within the study area and used a full-factorial three-factor ANOVA to partition the variance among the effects of time period, fuel scenario, fire-regime scenario, GCM, and residual spatial variation (representing differences across fire zones) on change in burn probability.

Projected changes in upland vegetation composition for each scenario were assessed based on a summarization of generalized cover types—grassland, deciduous woodland, mixedwood forest, and coniferous forest (Table 2)—by time period and GCM (Objectives 3 and 4). For fire-mediated scenarios, results were averaged over 10 fuel iterations per time period and GCM.

Results

Predicted vegetation

Our random forest model predicted 52% of Alberta to be composed of vegetated natural uplands (Appendix S1). Within our northern Alberta study area, 57% (247,895 km^2) was composed of vegetated natural uplands and 28% (123,112 km^2) was natural wetlands with an OOB classification error rate for the ecosite model of 20%. Of the natural uplands, 83.5% were predicted to fall within the medium-mesic moisture/nutrient category (11% OOB error rate). Predicted upland vegetation within the study area amounted to 26.5% conifer, 64.3% boreal mixedwood, 9.0% deciduous, and <0.1% grassland. The OOB error rate for 40 vegetation types was 19% (accuracy = 81%); aggregated to FBP system fuel type, the error rate was 11%. Additional model accuracy results and predictions are described in Appendix S1.

Fire simulation

Across all scenarios, simulated burn probability at a given pixel across 3000 iterations increased over time, especially for unconstrained fire regime scenarios (Fig. 3, Appendix S3: Fig. S1). With constrained fire regimes, static-fuel scenarios increased monotonically, whereas fire-mediated and climate-driven scenarios exhibited a mid-century decrease in the number of fires, increasing again by the end of the century (more rapidly for climate-driven fuel scenarios; Fig. 4).

The largest source of variation (proportion of total sum of squares) in burn probability was future time period (0.39), followed by fire regime (0.36), GCM (0.10), and the interaction between fire regime and time period (0.10; Table 3). Other sources of variation were small across all scenarios, but differences among fuel scenarios were apparent under constrained fire regimes (Fig. 4).

With respect to the two manipulated fire-regime components (number-of-escaped-fires and spread-day distributions), the number of escaped fires had a larger effect on the total area burned in the northernmost Great Slave Lake fire zone, while the number of spread days had a larger effect in the Southern Cordillera and Southern Prairies zones (Appendix S2: Table S3). The two different components were largely additive in terms of their influence, although the combined effects were greater than the sum their parts in the Southern Prairies zone, and slightly less in the other two zones.

Forest composition

Under climate-driven change scenarios, dramatic changes in vegetation types were projected for the next century (Appendix S3: Figs. S2, S3), with a nearly 250,000-km^2 increase in grassland area projected by the end of the century for all GCMs (Fig. 5). Climatic potential for upland

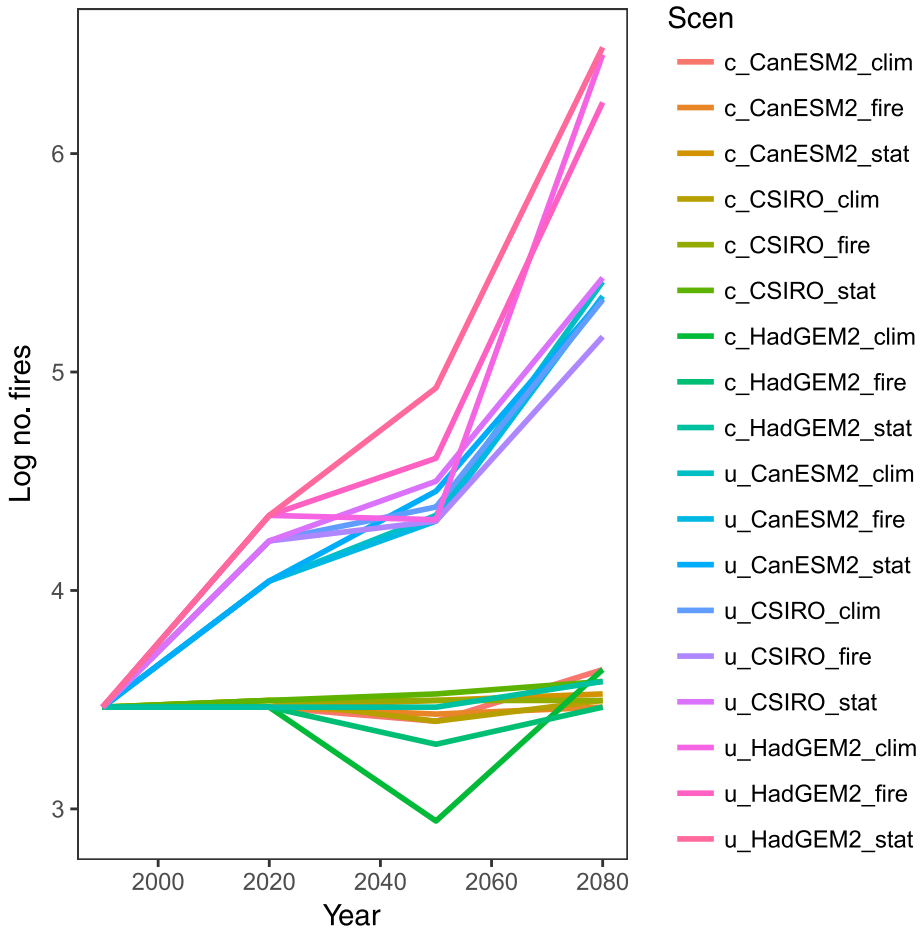

Fig. 3. Simulated median number of fires (log scale) over 3000 iterations for all scenarios. Burn probability = number of fires /3000; c = constrained fire regime; u = unconstrained fire regime; CanESM2, CSIRO, and HadGEM are different global climate models; clim = climate-driven fuels, fire = fire-mediated fuels, stat = static fuels.

conifer, mixedwood forest, and deciduous woodland was projected to decrease by ~62,000 km^2 (94%), ~156,000 km^2 (98%), and ~21,000 km^2 (96%) on average, respectively, by the end of the century (Fig. 5). Grassland potential increased and conifer and mixedwood potential decreased fairly steadily across GCMs, whereas deciduous projections fluctuated more and were less consistent across GCMs. Wetland vegetation types were held constant by design and thus did not change. As a result, there was little opportunity for upslope or northward movement of upland conifer vegetation types. Instead, change in conifer and mixedwood vegetation types was primarily a matter of contraction in area.

Vegetation projections from the fire-mediated scenarios were less extreme in comparison with the climate-driven scenarios, especially under constrained fire regimes (Figs. 6, 7). Under these scenarios, upland conifer and mixedwood forest were projected to decrease by <50% on average, whereas deciduous woodland was projected to increase rather than decrease, and grassland increases were less than half of the climate-mediated projections (Fig. 5). The unconstrained fire-regime scenario projections (Appendix S3: Fig. S4) were generally intermediate to the climate-driven and constrained fire-regime scenarios, resulting in a much smaller divergence from the climate-driven scenario (Fig. 5; Appendix S3: Fig. S5).

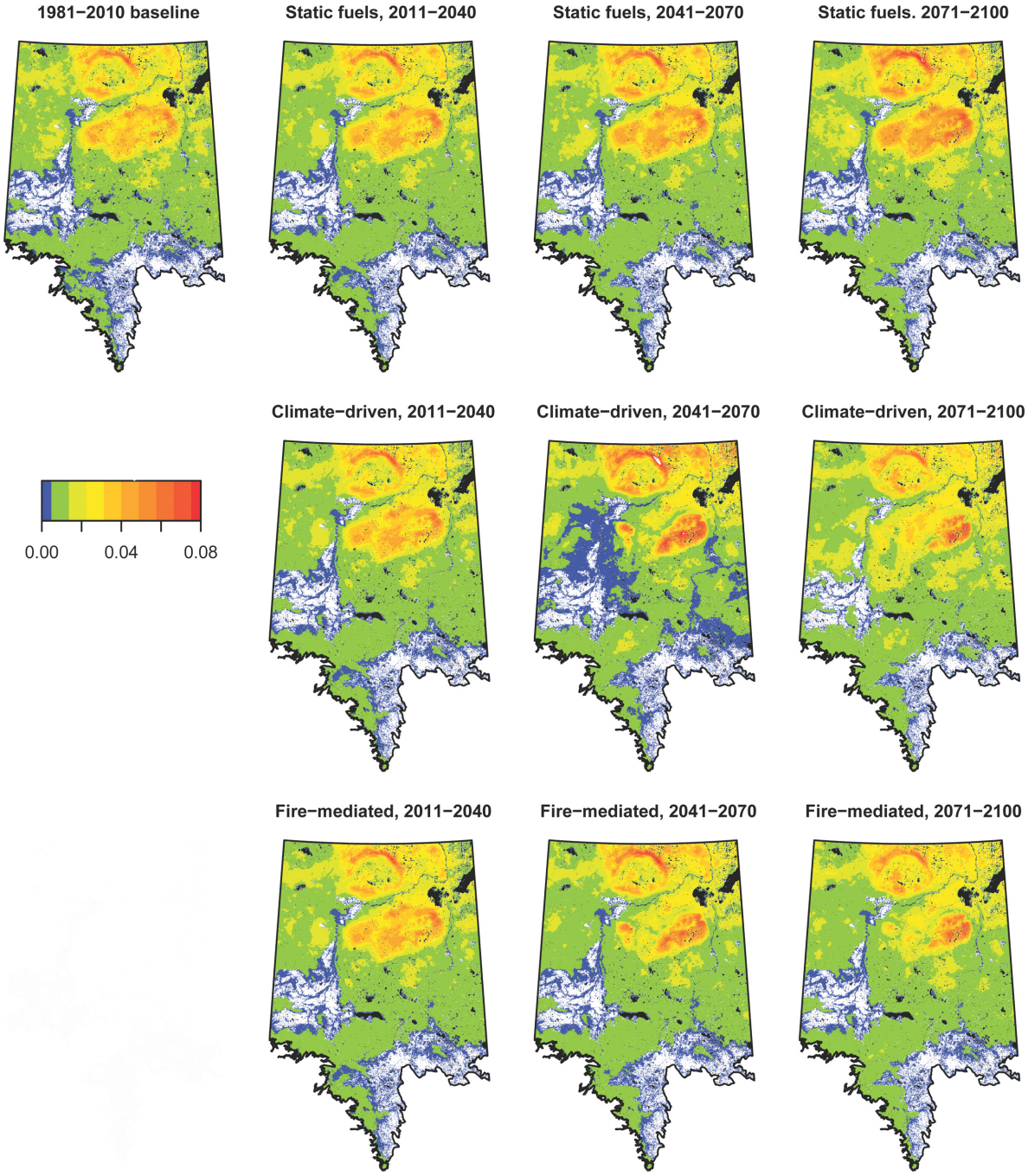

Fig. 4. Mean burn probability for each time period and fuel scenario, based on a constrained future fire regime. Burn probabilities were averaged across 3000 iterations. White areas represent nonfuel types.

Discussion

The speed at which ecosystems will respond to climate change within upcoming decades is a subject of great importance for climate-change adaptation and planning, yet still subject to great uncertainty. This is particularly true in the boreal forest of western North America, where an

Table 3. Proportional deviance contributions for projected burn probability, based on 900 regularly spaced sample points.

Variance component	Proportion
Fuel	0.002
Fire regime	0.361
Time period	0.387
GCM	0.096
Fuel × Fire regime	0.000
Fuel × Time period	0.001
Fire regime × Time period	0.095
Fuel × GCM	0.001
Fire regime × GCM	0.024
Time period × GCM	0.027
Fuel × Fire regime × Time period	0.000
Fuel × Fire regime × GCM	0.000
Fuel × Time period × GCM	0.000
Fire regime × Time period × GCM	0.006
Fuel × Fire regime × Time period × GCM	0.006
Spatial variation	0.360

Note: Values are proportions of explained deviance based on a Poisson generalized linear model with four time periods, three fuel scenarios, two fire-regime scenarios, and three global climate models (GCM).

already-dry climate is on the cusp of being unsuitable for widespread forest-dominated vegetation (Hogg and Hurdle 1995, Price et al. 2013, Gauthier et al. 2015) and the potential for large wildfires is almost certain to increase substantially (Flannigan et al. 2001, Balshi et al. 2009, Boulanger et al. 2014). We used a novel hybrid modeling approach based on topo-edaphically constrained projections of climate-driven vegetation change potential, coupled with weather- and fuel-based simulations of future wildland fire activity, to address this issue for upland forests in Alberta. Our simulations demonstrated how climate-driven changes in upland boreal forest vegetation could be delayed if disturbance is necessary to initiate vegetation transitions, as has been suggested previously (Schneider et al. 2009). Nevertheless, we found that if our conservative, constrained fire-regime projections are borne out, approximately a one-half reduction in the area of upland mixedwood and conifer forest (ranging from approximately one- to two-thirds), accompanied by an increase in grassland, should be anticipated by 2100, with net changes in deciduous forest depending on GCM. Under an unconstrained fire regime, extremely fire-conducive weather conditions could increase fire-mediated vegetation transitions to a level approaching the future climatic potential, resulting in a near-complete replacement of upland forest with grassland-dominated systems.

Climate-driven changes in vegetation

Projections from our topo-edaphically constrained empirical model suggested the potential for dramatic climate-driven changes in vegetation by the end of the 21st century. If disturbance were not required for vegetation transitions to occur, our models would indicate the potential for more than 95% of current upland conifer, mixedwood, and deciduous forests to be replaced by grassland, or novel grassland-dominated ecosystems that still retain trees and other forest elements. Substantial variation among GCMs was only evident in projections for deciduous forest. This is generally in line with other high-end (~1000 ppm CO_2 equivalent) projections for the region (Schneider 2013, Rooney et al. 2015), as well as pollen records suggesting that the current boreal region may have been grassland-dominated during the warmer (by 2°C) Hypsithermal period, 9000 to 6000 yr before present (Strong and Hills 2003), and contained substantially more graminoids during the Medieval Warm period ~500 yr ago (Larsen and MacDonald 1998). Our incorporation of topo-edaphic constraints resulted in particularly dramatic projected losses of upland forest, however. If wetlands do indeed persist in their current locations as we assumed, our simulations suggest a novel landscape juxtaposition of peatlands surrounded by deciduous forest and eventually grasslands over the next century, as discussed by Schneider et al. (2016). Indeed, peatland complexes, and to some extent, hydrologically connected uplands, may serve as hydrologic refuges under climate change (McLaughlin et al. 2017).

Based on this assumption that boreal wetland vegetation will remain static over the next century, upslope migration of boreal upland conifer and mixedwood forest will likely be constrained by large permafrost wetland complexes at higher elevations (Schneider et al. 2016) and additionally affected by near-term permafrost thaw dynamics (Baltzer et al. 2014). Paradoxically, we found that the regions with greatest persistence probabilities for conifer and mixedwood forests were southern latitude foothill regions with lower rates of wildfire. Thus, in the absence of large-scale rapid permafrost melt and drying of

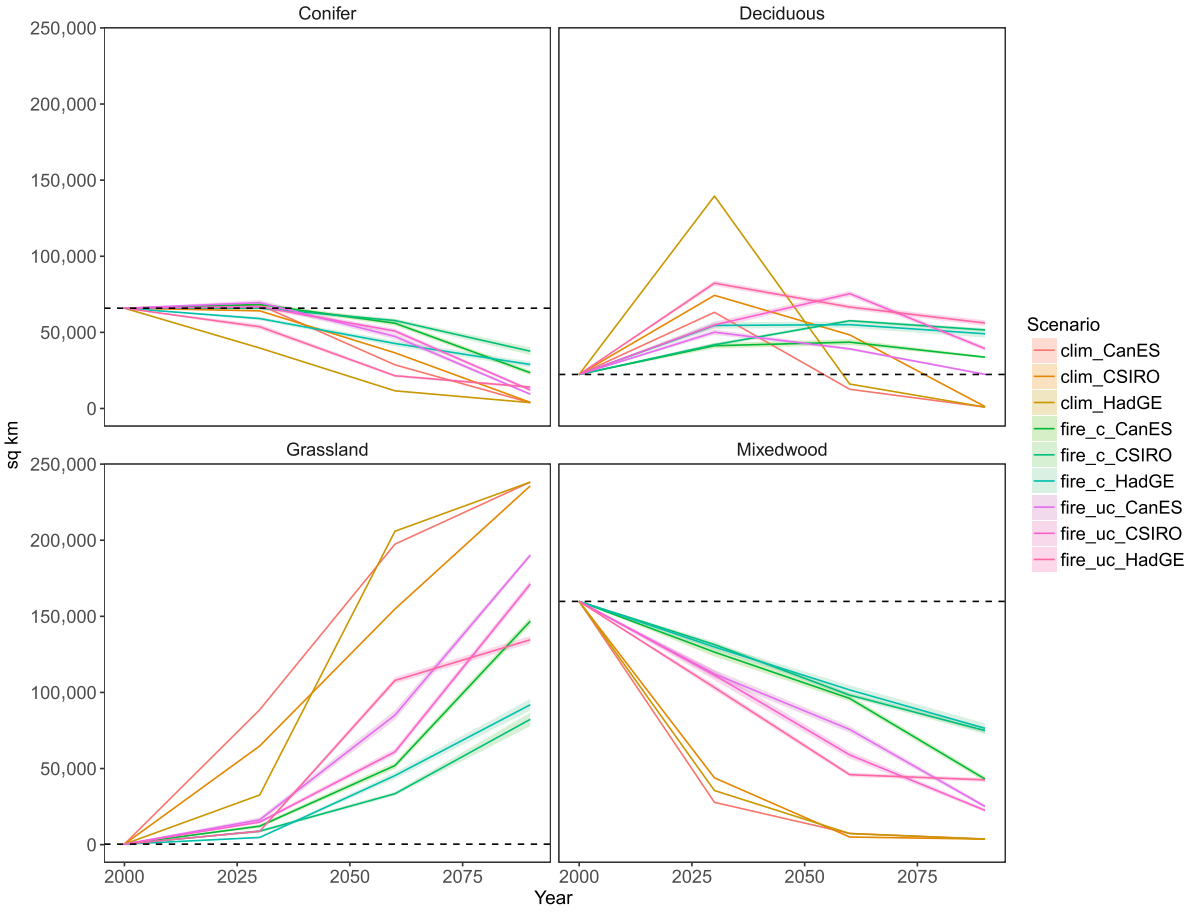

Fig. 5. Projected change in upland vegetation cover type over time by global climate model (GCM) and scenario. clim = climate-driven, fire_c = fire-mediated, constrained fire regime, fire_uc = fire-mediated, unconstrained fire regime. CanES (CanESM2), CSIRO, and HadGE (HadGEM) represent different GCMs. Dashed line represents no change scenario. Forest area units are km^2.

peatlands, upland conifer and mixedwood species in Alberta may be dependent on fire refugia —that is, "places that are disturbed less frequently or less severely by wildfire than the surrounding landscape matrix" (Krawchuk et al. 2016), based primarily on topography and isolation (e.g., lakeshores and islands, Nielsen et al. 2016). Due to the relatively coarse (500-m) resolution of inputs, our simulation did not lend itself to the identification of local fire refugia. For this, finer-scale simulations will be necessary.

Alternatively, and over the long term, forest-associated species may rely heavily on northward expansions in the Northwest Territories and Yukon Territory, but such vegetation transitions are also constrained by permafrost wetland dynamics (Lara et al. 2016), soil development limitations, and mountain geometry (Elsen and Tingley 2015). Thus, in contrast with the traditional paradigm of faster rates of climate-change response on the leading edge of species' distributions where competition is reduced (Ordonez and Williams 2013), the situation may be reversed in the western boreal region. That is, northern and elevational shifts are constrained by wetlands that are likely to persist longer than upland habitats. Meanwhile, southern margins along the boreal-grassland ecotone are most vulnerable to changes in available moisture and associated tree mortality (Michaelian et al. 2010), exacerbated by anthropogenic landscape fragmentation, resulting in low "vegetation

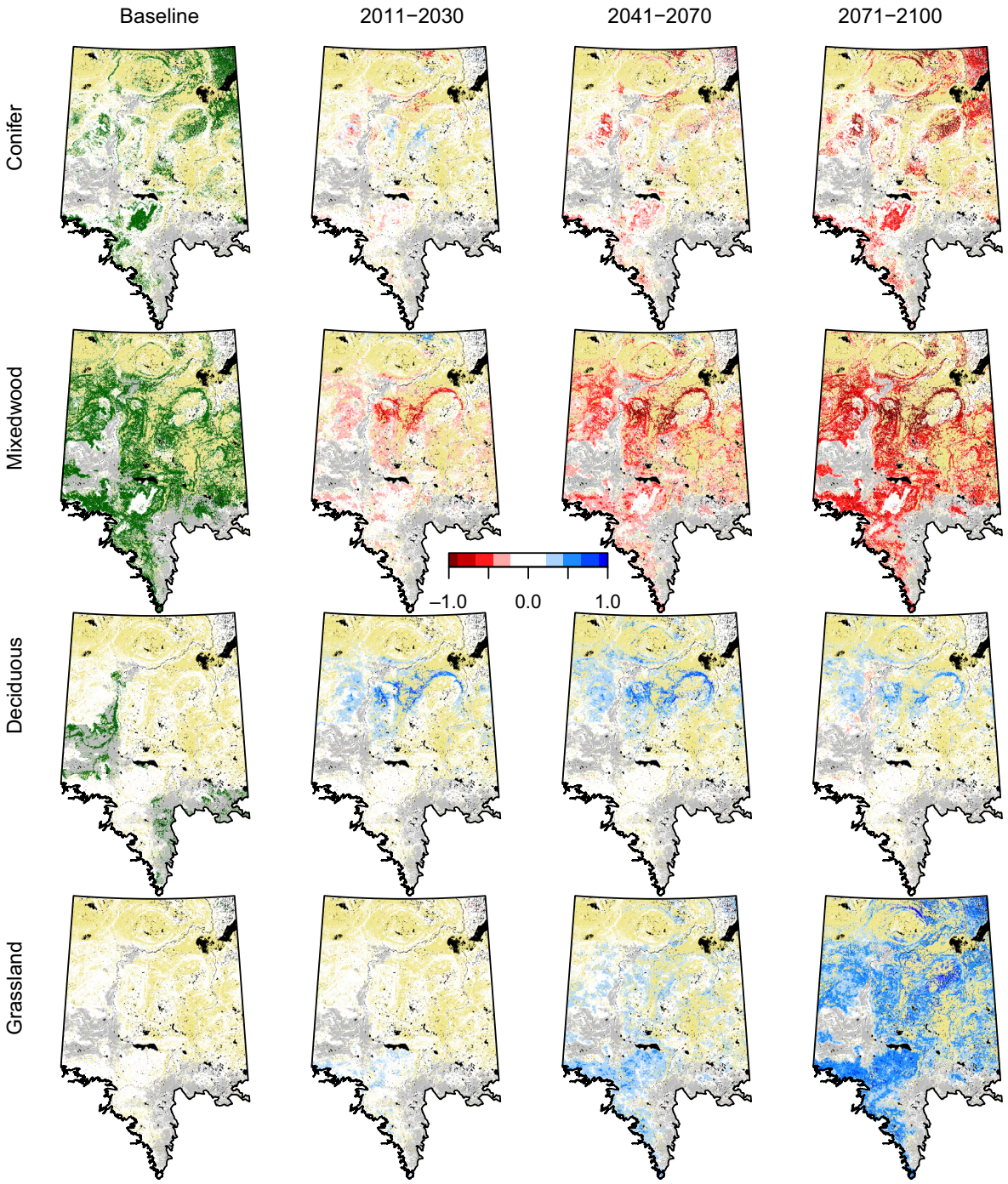

Fig. 6. Predicted proportional change (blue = increasing, red = decreasing) in conifer, mixedwood, deciduous, and grassland vegetation types for current and three future time periods under a fire-mediated scenario based on a constrained fire regime (blue = increasing, red = decreasing). Proportions based on 10 fuel realizations × 3 global climate models. Baseline modeled vegetation shown in green in first column. Black = open water; gray = nonfuel; beige = wetland vegetation.

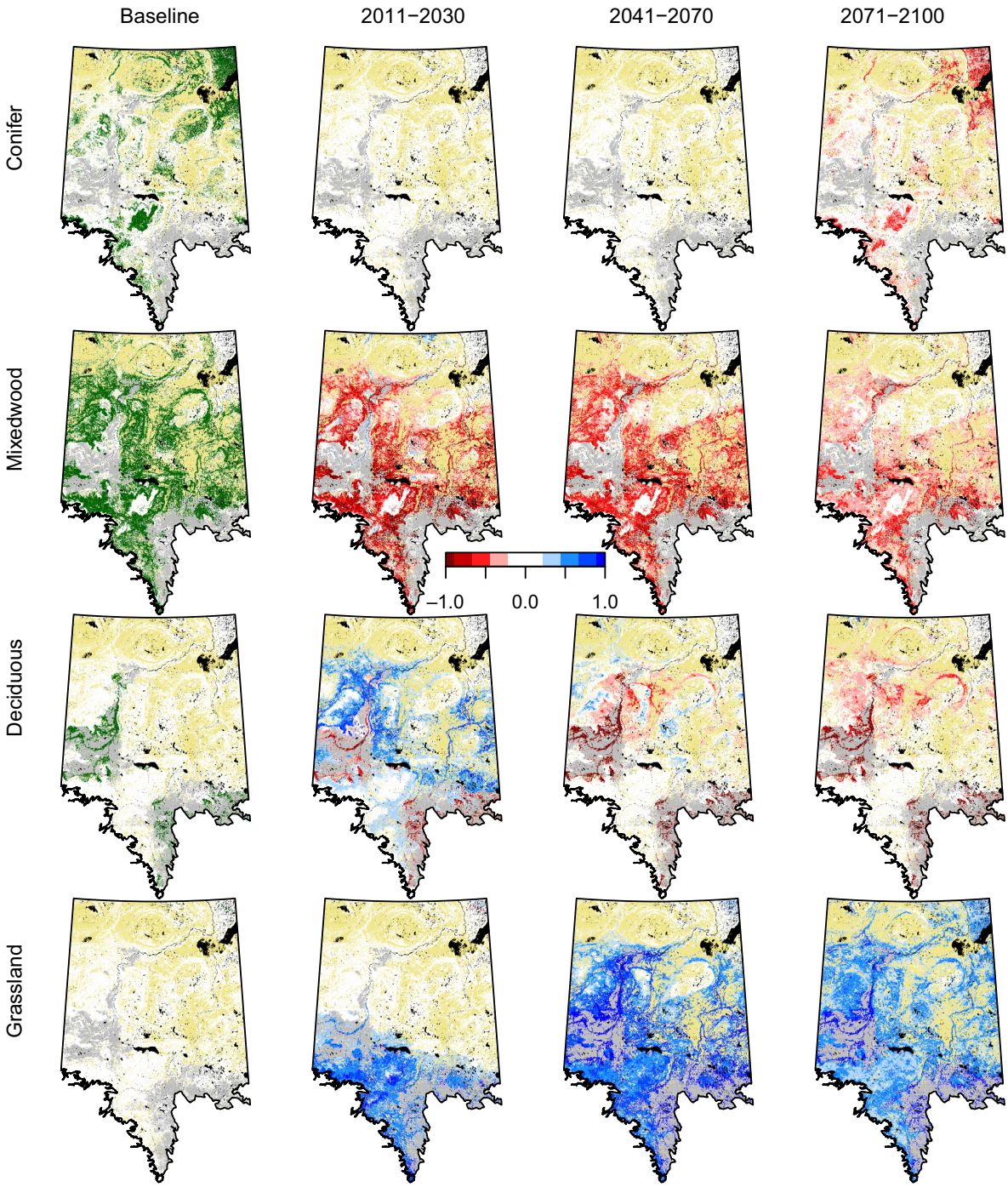

Fig. 7. Difference between climate-driven and fire-mediated proportional change (blue = larger increase, red = larger decrease) in conifer, mixedwood, deciduous, and grassland vegetation types for three future time periods under a fire-mediated scenario based on a constrained fire regime. Proportions based on 10 fuel realizations × 3 global climate models. Baseline modeled vegetation shown in green in first column. Black = open water; gray = nonfuel; beige = wetland vegetation.

intactness" (Watson et al. 2013). Thus, forest retreats along the southern edge could happen faster than advances along northern margins.

Fire-mediated vegetation projections

Imposing fire-mediated vegetation transitions yielded considerably slower rates of change compared to purely climate-driven projections. This was especially true under the constrained fire-regime scenarios, for which our simulations suggest a negative feedback process by which a warmer climate and more extensive near-term fires lead to an increase in deciduous forest (dominated by trembling aspen, *Populus tremuloides*) that in turn, due to its relatively low flammability, leads to a long-term reduction in area burned (Terrier et al. 2012). Under current warming trajectories, however, such states may be short-lived or depend on human intervention to be maintained. By the end of the century, as grasslands were projected to become more prevalent, our simulated burn probabilities increased accordingly. This temporary reduction in fire activity, in spite of increases in extreme fire weather conditions (Wang et al. 2015), reflects the important influence of vegetation composition (i.e., fuels) on wildfire occurrence, at least under modern-day fire regimes. It is consistent with Wang et al. (2016), who also found a projected decrease in burn probability over time in the western interior forests of British Columbia, Canada, where an increase in fire-conducive weather had a modest influence on fire likelihood compared to that of reduced fuel flammability.

With an unconstrained fire regime, however, the weather-driven increase in fires more than compensated for the reduction in fuel flammability, and fire activity increased dramatically regardless of fuel scenario, driving a rapid climatic transition to grass-dominated systems. Despite low biomass, grasses provide highly flammable fuels when dry (Thompson et al. 2017*b*). Within a forested landscape, increased grassland prevalence may facilitate wildfire ignition and spread (Gartner et al. 2012), in contrast to deciduous forest (Parisien et al. 2011*b*). Furthermore, the high prevalence of interspersed boreal wetlands can also facilitate fire spread, with rapid accumulation of highly flammable fuels (Thompson et al. 2017*b*). Thus, in the absence of fire suppression, eventual grass- and wetland-dominated landscapes could experience a higher frequency of fire than parts of the current boreal forest mosaic. Although we did not directly examine severity due to computational constraints, a grass-dominated fire regime would likely be comprised of lower-severity fires rather than high-severity crown fires, which is currently the norm (Whitman et al. 2018). Possible current analogs may be found in highly flammable grass-understory pine forests of the interior western United States and British Columbia (Arno 1980, Veblen et al. 2000), or potentially in the open, larch- and pine-dominated forests of Siberia (de Groot et al. 2013).

Sources of uncertainty

The wide range of possible future outcomes that we found highlights the high levels of uncertainty associated with future vegetation trajectories in the highly dynamic boreal forest region of Alberta. Overall, the largest source of variation in burn probability was fire regime (specifically, number and duration of fires), closely followed by directional changes in climate (i.e., increases in fire-conducive weather) over time and differences among fire zones. Global climate model-related uncertainty in burn probability was substantial, but swamped by directional changes in climate, consistent with various correlative model predictions for this region (Stralberg et al. 2015, Boulanger et al. 2016*a*, but see Boulanger et al., *in press*).

On the one hand, our constrained fire regime, which assumes that current fire characteristics remain constant, may be unrealistically conservative as extreme fire weather conditions increase (although reduced fuel flammability could eventually make it too extreme). On the other hand, our unconstrained fire-regime scenario is undoubtedly too extreme over the long term, given Burn-P3's largely additive treatment of different fire-regime components (spread duration and number of fires). Although climatic controls on various components of some existing boreal (Boulanger et al. 2012) and western mountain (Whitman et al. 2015) fire regimes have been described, there is insufficient information about future fire regimes to inform more moderate scenarios (Williams and Abatzoglou 2016). This is largely due to the widespread disequilibrium between climate and fuels that is anticipated in upcoming decades, resulting in no-analog fire environments.

Our study has highlighted substantial knowledge gaps that should be addressed before we can claim to make accurate projections of future fire activity in the boreal forest. Perhaps the most important of these gaps is the lack of understanding of how long fires will burn in fire environments that have no current analogs (Wang et al. 2017). The duration of burning can have a dramatic effect on fire sizes due to the fact that wildfire growth follows a power function over time (Van Wagner 1969). In other words, small changes in duration can lead to disproportionally large changes in final fire size. While our estimates of future fire-regime parameters were strictly a function of weather, changing vegetation types and landscape configurations (Miller and Urban 2000, O'Donnell et al. 2011, Marchal et al. 2017) will undoubtedly play a role. Evaluating the effects of these factors on potential fire duration is thus a critical step in improving future projections of fire activity. For example, a regime consisting largely of grass-fueled surface fires could emerge in Alberta as forests become more open and grass-dominated. In that case, our spread-day (duration) projections would be overestimates, given the lower potential for combustion to persist in low-soil biomass grasslands than in forest stands. Conversely, our projections for the number of escaped fires could be underestimates, depending on the wetland portion of the fuel mosaic.

Caveats and limitations

Fire-regime parameters aside, our fire-mediated, constrained fire-regime scenarios for vegetation change were conservative in the sense that they do not account for continued future increases in drought, insect defoliation, or anthropogenic disturbances that can also result in reduced tree growth (Girardin et al. 2008, Hogg et al. 2017) and increased tree mortality (Allen et al. 2010, 2015, Zhang et al. 2015), further facilitating ecosystem transitions. The static treatment of wetland vegetation was also a conservative assumption that was deemed more plausible than the alternative option (climatic modeling and projection of wetland vegetation types). Although some lag in boreal peatland conversion appears inevitable (Schneider et al. 2016), there is high uncertainty about rates of change (Camill and Clark 2000). Scenarios of rapid drying, due to a lowering of the water table, are also possible (Turetsky et al. 2015, Thompson et al. 2017*a*) and would lead to more dramatic vegetation changes, but also greater potential for encroachment and persistence of upland forest types.

Climatically, however, our projections may have been too extreme with respect to climate-change projections in the Rocky Mountain Foothills and central highlands. Our vegetation model projects a large climate-driven conversion to grasslands within this region, as do other models specific to Alberta or western North America (Schneider et al. 2009, Mbogga et al. 2010). Yet future climate projections suggest that it will retain a moisture surplus in the future (Schneider et al. 2003); thus, an increase in temperature may not result in a conversion to the grassland systems found in warmer portions of Alberta. Other continental-scale analyses suggest that the foothills climate regime could more closely resemble that of eastern deciduous forests in terms of vegetation (Rehfeldt et al. 2012) and passerine birds (Stralberg et al. 2015), but with a high probability that future conditions will have no contemporary analog (Rehfeldt et al. 2012, Mahony et al. 2017).

Finally, our empirical vegetation model was relatively simplistic in that it did not consider stand age or successional stage. As such, some vegetation types, such as medium-mesic white spruce and aspen, may have been driven by site disturbance history and forest age rather than climate or topo-edaphic conditions, thereby reducing the precision of our models. Alberta has a clear north–south human disturbance gradient, which could have partially confounded the influence of climate on vegetation type, potentially increasing the magnitude of projected climate-driven vegetation change. However, the ABMI vegetation dataset upon which our model relies includes many off-grid sites that were selected specifically to reduce the correlation between latitude and anthropogenic disturbance. Thus, we concluded that any such bias would be minor.

Conclusion

While climate-change uncertainty is formidable, the ability to anticipate alternative future change timelines and trajectories will be invaluable to climate-change adaptation and conservation planning efforts. Model generality and

simplicity are prized in many circumstances. However, the magnitude and scope of anthropogenic climate change, along with the potential for nonanalog conditions and prolonged states of disequilibrium, suggests the need for novel, hybrid modeling approaches that address critical local dynamic processes while considering a spatial scale broad enough to capture the range of anticipated future variability (Gustafson 2013, Williams and Abatzoglou 2016). We have presented such an approach for the western boreal region of North America, where it is impossible to consider future climate change in isolation from wildfire, and where topo-edaphic legacies have major influences on biota that are not captured with equilibrium climate models. Our ecosite-based model, combined with fire-mediated vegetation transitions, provides a moderated range of estimates for future vegetation in boreal Alberta, but suggests ample opportunity for fire (and other disturbance) to facilitate rapid vegetation change, approaching its future climatic potential. To accommodate change while preserving boreal ecosystems and resources, managers should prepare for rapid transitions and protect higher-elevation refuges and large peatland complexes in which boreal forest systems are most likely to persist. Meanwhile, models should continue to be refined as the relationships between fire, climate, and fuels become better understood. Contingent upon proper parameterization, our model framework may also be applied to other circumboreal regions—and even other fire-prone biomes—in order to evaluate the generality of these findings.

Acknowledgments

This project was made possible by data from the Alberta Biodiversity Monitoring Institute (ABMI), Environment Canada, Natural Resources Canada, and Alberta Environment and Parks (Ecosite Information System). Funding for this project was provided by the Climate Change Emissions Management Corporation, the University of Alberta, NSERC, Alberta Innovates, Alberta Conservation Association, and ABMI. Diana Stralberg was also supported by the Boreal Avian Modelling Project (borealbirds.ca) and the AdaptWest Climate Adaptation Planning Project (adaptwest.databasin.org). We are grateful for various forms of assistance from Harry Archibald, Craig Aumann, Matt Carlson, Easwaramurthyvasi Chidambaravasi, Jacqueline Dennett, QiongYan Fang, Dan Farr, Trish Fontaine, Tom Habib, Melynda Johnson, Hedwig Lankau, Suzanne Lavoie, Amy Nixon, Daiyuan Pan, Wayne Pettapiece, Jim Schieck, Rick Schneider, Brian Simpson, Jessica Stolar, Cassidy van Rensen, and Mike Willoughby. Manuscript division of labor can be described as follows: DS and EMB conceived of the paper; DS, XW, MAP, and FNR designed and executed the fire simulation component; PS, CLM, SEN, and EMB contributed data and expertise for vegetation modeling; DS conducted vegetation modeling and wrote the paper; all co-authors contributed to paper review and revision.

Literature Cited

Allen, C. D., D. D. Breshears, and N. G. McDowell. 2015. On underestimation of global vulnerability to tree mortality and forest die-off from hotter drought in the Anthropocene. Ecosphere 6:art129.

Allen, C. D., et al. 2010. A global overview of drought and heat-induced tree mortality reveals emerging climate change risks for forests. Forest Ecology and Management 259:660–684.

Anderson, K. 2010. A climatologically based long-range fire growth model. International Journal of Wildland Fire 19:879–894.

Arno, S. F. 1980. Forest fire history in the Northern Rockies. Journal of Forestry 78:460–465.

Balshi, M. S., A. D. McGuire, P. Duffy, M. Flannigan, J. Walsh, and J. Melillo. 2009. Assessing the response of area burned to changing climate in western boreal North America using a Multivariate Adaptive Regression Splines (MARS) approach. Global Change Biology 15:578–600.

Baltzer, J. L., T. Veness, L. E. Chasmer, A. E. Sniderhan, and W. L. Quinton. 2014. Forests on thawing permafrost: fragmentation, edge effects, and net forest loss. Global Change Biology 20:824–834.

Bernier, P. Y., S. Gauthier, P.-O. Jean, F. Manka, Y. Boulanger, A. Beaudoin, and L. Guindon. 2016. Mapping local effects of forest properties on fire risk across Canada. Forests 7:1–11.

Boulanger, Y., S. Gauthier, and P. J. Burton. 2014. A refinement of models projecting future Canadian fire regimes using homogeneous fire regime zones. Canadian Journal of Forest Research 44:365–376.

Boulanger, Y., S. Gauthier, P. J. Burton, and M.-A. Vaillancourt. 2012. An alternative fire regime zonation for Canada. International Journal of Wildland Fire 21:1052–1064.

Boulanger, Y., D. R. Gray, B. J. Cooke, and L. De Grandpré. 2016*a*. Model-specification uncertainty in future forest pest outbreak. Global Change Biology 22:1595–1607.

Boulanger, Y., M.-A. Parisien, and X. Wang. *In press*. Model-specification uncertainty in future area burned by wildfires in Canada. International Journal of Wildland Fire http://www.publish.csiro.au/WF/justaccepted/WF17123

Boulanger, Y., A. R. Taylor, D. T. Price, D. Cyr, E. McGarrigle, W. Rammer, G. Sainte-Marie, A. Beaudoin, L. Guindon, and N. Mansuy. 2016*b*. Climate change impacts on forest landscapes along the Canadian southern boreal forest transition zone. Landscape Ecology 32:1–17.

Boutin, S., D. L. Haughland, J. Schieck, J. Herbers, and E. Bayne. 2009. A new approach to forest biodiversity monitoring in Canada. Forest Ecology and Management 258(Supplement):S168–S175.

Breiman, L. 2001. Random forests. Machine Learning 45:5–32.

Camill, P., and J. S. Clark. 2000. Long-term perspectives on lagged ecosystem responses to climate change: permafrost in boreal peatlands and the grassland/woodland boundary. Ecosystems 3:534–544.

Canadian Forest Service. 2015. Canadian national fire database. Natural Resources Canada, Canadian Forest Service, Northern Forestry Centre, Edmonton, Alberta, Canada. [online] http://cwfis.cfs.nrcan.gc.ca/ha/nfdb

Chylek, P., J. Li, M. K. Dubey, M. Wang, and G. Lesins. 2011. Observed and model simulated 20th century Arctic temperature variability: Canadian Earth System Model CanESM2. Atmospheric Chemistry and Physics Discussions 2011:22893–22907.

Cumming, S. G. 2001. Forest type and wildfire in the Alberta boreal mixedwood: What do fires burn? Ecological Applications 11:97–110.

Cushman, S. A., D. McKenzie, D. L. Peterson, J. Littell, and K. S. McKelvey. 2006. Research agenda for integrated landscape modeling. USDA Forest Service Gen. Tech. Rep. RMRS-194. Rocky Mountain Research Station, Fort Collins, Colorado, USA. https://www.fs.usda.gov/treesearch/pubs/27437

Cyr, D., S. Gauthier, Y. Bergeron, and C. Carcaillet. 2009. Forest management is driving the eastern North American boreal forest outside its natural range of variability. Frontiers in Ecology and the Environment 7:519–524.

de Groot, W. J., A. S. Cantin, M. D. Flannigan, A. J. Soja, L. M. Gowman, and A. Newbery. 2013. A comparison of Canadian and Russian boreal forest fire regimes. Forest Ecology and Management 294:23–34.

Elsen, P. R., and M. W. Tingley. 2015. Global mountain topography and the fate of montane species under climate change. Nature Climate Change 5:772–776.

Flannigan, M. D., B. D. Amiro, K. A. Logan, B. J. Stocks, and B. M. Wotton. 2006. Forest fires and climate change in the 21st century. Mitigation and Adaptation Strategies for Global Change 11:847–859.

Flannigan, M., I. Campbell, M. Wotton, C. Carcaillet, P. Richard, and Y. Bergeron. 2001. Future fire in Canada's boreal forest: paleoecology results and general circulation model—regional climate model simulations. Canadian Journal of Forest Research 31:854–863.

Flannigan, M. D., M. A. Krawchuk, W. J. de Groot, B. M. Wotton, and L. M. Gowman. 2009. Implications of changing climate for global wildland fire. International Journal of Wildland Fire 18:483–507.

Flannigan, M., K. Logan, B. Amiro, W. Skinner, and B. Stocks. 2005. Future area burned in Canada. Climatic Change 72:1–16.

Forestry Canada Fire Danger Group. 1992. Development and structure of the Canadian Forest Fire Behavior Prediction System. Information Report ST-X-3. Canadian Forest Service, Ottawa, Ontario, Canada. https://cfs.nrcan.gc.ca/publications?id=10068

Fuss, S., et al. 2014. Betting on negative emissions. Nature Climate Change 4:850–853.

Gartner, M. H., T. T. Veblen, R. L. Sherriff, and T. L. Schoennagel. 2012. Proximity to grasslands influences fire frequency and sensitivity to climate variability in ponderosa pine forests of the Colorado Front Range. International Journal of Wildland Fire 21:562–571.

Gauthier, S., P. Bernier, T. Kuuluvainen, A. Z. Shvidenko, and D. G. Schepaschenko. 2015. Boreal forest health and global change. Science 349:819–822.

Girardin, M. P., F. Raulier, P. Y. Bernier, and J. C. Tardif. 2008. Response of tree growth to a changing climate in boreal central Canada: a comparison of empirical, process-based, and hybrid modelling approaches. Ecological Modelling 213:209–228.

Gustafson, E. 2013. When relationships estimated in the past cannot be used to predict the future: using mechanistic models to predict landscape ecological dynamics in a changing world. Landscape Ecology 28:1429–1437.

Hauer, G., S. Cumming, F. Schmiegelow, W. Adamowicz, M. Weber, and R. Jagodzinski. 2010. Tradeoffs between forestry resource and conservation values under alternate policy regimes: a spatial analysis of the western Canadian boreal plains. Ecological Modelling 221:2590–2603.

Héon, J., D. Arseneault, and M.-A. Parisien. 2014. Resistance of the boreal forest to high burn rates.

Proceedings of the National Academy of Sciences of the United States of America 11:13888–13893.

Hickler, T., et al. 2012. Projecting the future distribution of European potential natural vegetation zones with a generalized, tree species-based dynamic vegetation model. Global Ecology and Biogeography 21:50–63.

Hogg, E. H. 1994. Climate and the southern limit of the western Canadian boreal forest. Canadian Journal of Forest Research 24:1835–1845.

Hogg, E. H., J. P. Brandt, and B. Kochtubajda. 2002. Growth and dieback of aspen forests in northwestern Alberta, Canada, in relation to climate and insects. Canadian Journal of Forest Research 32:823–832.

Hogg, E. H., and P. A. Hurdle. 1995. The aspen parkland in western Canada: A dry-climate analogue for the future boreal forest? Water, Air, & Soil Pollution 82:391–400.

Hogg, E. H., M. Michaelian, T. I. Hook, and M. E. Undershultz. 2017. Recent climatic drying leads to age-independent growth reductions of white spruce stands in western Canada. Global Change Biology 23:5297–5308.

Hogg, E. H., and A. G. Schwarz. 1997. Regeneration of planted conifers across climatic moisture gradients on the Canadian prairies: implications for distribution and climate change. Journal of Biogeography 24:527–534.

Hurrell, J. W., et al. 2013. The community earth system model: a framework for collaborative research. Bulletin of the American Meteorological Society 94:1339–1360.

Jarvis, A., H. I. Reuter, A. Nelson, and E. Guevara. 2008. Hole-filled seamless SRTM data V4, International Centre for Tropical Agriculture (CIAT). http://srtm.csi.cgiar.org

Johnstone, J. F., T. N. Hollingsworth, F. S. Chapin, and M. C. Mack. 2010. Changes in fire regime break the legacy lock on successional trajectories in Alaskan boreal forest. Global Change Biology 16:1281–1295.

Jones, C. D., et al. 2011. The HadGEM2-ES implementation of CMIP5 centennial simulations. Geoscientific Model Development 4:543–570.

Kasischke, E. S., and M. R. Turetsky. 2006. Recent changes in the fire regime across the North American boreal region—spatial and temporal patterns of burning across Canada and Alaska. Geophysical Research Letters 33:L09703.

Keane, R. E., G. J. Cary, I. D. Davies, M. D. Flannigan, R. H. Gardner, S. Lavorel, J. M. Lenihan, C. Li, and T. S. Rupp. 2004. A classification of landscape fire succession models: spatial simulations of fire and vegetation dynamics. Ecological Modelling 179: 3–27.

Krawchuk, M., S. Cumming, and M. Flannigan. 2009. Predicted changes in fire weather suggest increases in lightning fire initiation and future area burned in the mixedwood boreal forest. Climatic Change 92:83–97.

Krawchuk, M. A., S. L. Haire, J. Coop, M.-A. Parisien, E. Whitman, G. Chong, and C. Miller. 2016. Topographic and fire weather controls of fire refugia in forested ecosystems of northwestern North America. Ecosphere 7:e01632.

Lara, M. J., H. Genet, A. D. McGuire, E. S. Euskirchen, Y. Zhang, D. R. N. Brown, M. T. Jorgenson, V. Romanovsky, A. Breen, and W. R. Bolton. 2016. Thermokarst rates intensify due to climate change and forest fragmentation in an Alaskan boreal forest lowland. Global Change Biology 22:816–829.

Larsen, C. P. S., and G. M. MacDonald. 1998. An 840-year record of fire and vegetation in a boreal white spruce forest. Ecology 79:106–118.

Luo, Y., and H. Y. H. Chen. 2013. Observations from old forests underestimate climate change effects on tree mortality. Nature Communications 4:1655.

Ma, Z., C. Peng, Q. Zhu, H. Chen, G. Yu, W. Li, X. Zhou, W. Wang, and W. Zhang. 2012. Regional drought-induced reduction in the biomass carbon sink of Canada's boreal forests. Proceedings of the National Academy of Sciences of the United States of America 109:2423–2427.

Mahony, C. R., A. J. Cannon, T. Wang, and S. N. Aitken. 2017. A closer look at novel climates: new methods and insights at continental to landscape scales. Global Change Biology 23:3934–3955.

Marchal, J., S. G. Cumming, and E. J. B. McIntire. 2017. Exploiting Poisson additivity to predict fire frequency from maps of fire weather and land cover in boreal forests of Québec, Canada. Ecography 40:200–209.

Mbogga, M. S., X. Wang, and A. Hamann. 2010. Bioclimate envelope model predictions for natural resource management: dealing with uncertainty. Journal of Applied Ecology 47:731–740.

McLaughlin, B. C., D. D. Ackerly, P. Z. Klos, J. Natali, T. E. Dawson, and S. E. Thompson. 2017. Hydrologic refugia, plants, and climate change. Global Change Biology 23:2941–2961.

Meier, E. S., H. Lischke, D. R. Schmatz, and N. E. Zimmermann. 2012. Climate, competition and connectivity affect future migration and ranges of European trees. Global Ecology and Biogeography 21:164–178.

Michaelian, M., E. H. Hogg, R. J. Hall, and E. Arsenault. 2010. Massive mortality of aspen following severe drought along the southern edge of the Canadian boreal forest. Global Change Biology 17:2084–2094.

Miller, C., and D. L. Urban. 2000. Connectivity of forest fuels and surface fire regimes. Landscape Ecology 15:145–154.

Natural Regions Committee. 2006. Natural Regions and Subregions of Alberta. Compiled by D.J. Downing and W.W. Pettapiece. Government of Alberta. Pub. No. T/852.

Nielsen, S., E. DeLancey, K. Reinhardt, and M.-A. Parisien. 2016. Effects of lakes on wildfire activity in the boreal forests of Saskatchewan, Canada. Forests 7:265.

O'Donnell, A. J., M. M. Boer, W. L. McCaw, and P. F. Grierson. 2011. Vegetation and landscape connectivity control wildfire intervals in unmanaged semi-arid shrublands and woodlands in Australia. Journal of Biogeography 38:112–124.

Ordonez, A., and J. W. Williams. 2013. Climatic and biotic velocities for woody taxa distributions over the last 16 000 years in eastern North America. Ecology Letters 16:773–781.

Pan, D., J. Schieck, and S. F. Morrison. 2014. 2000 Alberta backfilled wall-to-wall land cover Version 2.5 - Metadata. http://www.abmi.ca/home/publications/301-350/349.html

Parisien, M. A., V. G. Kafka, K. G. Hirsch, J. B. Todd, S. G. Lavoie, and P. D. Maczek. 2005. Mapping wildfire susceptibility with the BURN-P3 simulation model. Natural Resources Canada, Canadian Forest Service, Northern Forestry Centre, Edmonton, Alberta, Canada. https://cfs.nrcan.gc.ca/publications?id=25627

Parisien, M.-A., S. Parks, M. Krawchuk, M. Flannigan, L. Bowman, and M. Moritz. 2011*a*. Scale-dependent controls on the area burned in the boreal forest of Canada, 1980–2005. Ecological Applications 21:789–805.

Parisien, M.-A., S. Parks, C. Miller, M. Krawchuk, M. Heathcott, and M. Moritz. 2011*b*. Contributions of ignitions, fuels, and weather to the spatial patterns of burn probability of a boreal landscape. Ecosystems 14:1141–1155.

Peng, C., Z. Ma, X. Lei, Q. Zhu, H. Chen, W. Wang, S. Liu, W. Li, X. Fang, and X. Zhou. 2011. A drought-induced pervasive increase in tree mortality across Canada's boreal forests. Nature Climate Change 1:467–471.

Podur, J. J., and B. M. Wotton. 2011. Defining fire spread event days for fire-growth modeling. International Journal of Wildland Fire 20:497–507.

Price, D. T., et al. 2013. Anticipating the consequences of climate change for Canada's boreal forest ecosystems. Environmental Reviews 21:322–365.

Rehfeldt, G. E., N. L. Crookston, C. Sáenz-Romero, and E. M. Campbell. 2012. North American vegetation model for land-use planning in a changing climate: a solution to large classification problems. Ecological Applications 22:119–141.

Richards, G. D. 1995. A general mathematical framework for modeling two-dimensional wildland fire spread. International Journal of Wildland Fire 5:63–72.

Robinne, F.-N., M.-A. Parisien, and M. Flannigan. 2016. Anthropogenic influence on wildfire activity in Alberta, Canada. International Journal of Wildland Fire 25:1131–1143.

Rooney, R. C., D. T. Robinson, and R. Petrone. 2015. Megaproject reclamation and climate change. Nature Climate Change 5:963–966.

Schieck, J., P. Sólymos, and D. Huggard. 2014. Human Footprint in Alberta. ABMI Science Letters. Alberta Biodiversity Monitoring Institute, Edmonton, Alberta, Canada. http://www.abmi.ca/home/newsletters/scienceletter-past-issues.html

Schneider, R. 2013. Alberta's Natural Subregions under a Changing Climate. Alberta Biodiversity Monitoring Institute, Edmonton, Alberta, Canada. http://www.biodiversityandclimate.abmi.ca/#reports

Schneider, R., E. Bayne, and K. DeVito. 2016. Moving beyond bioclimatic envelope models: integrating upland forest and peatland processes to predict ecosystem transitions under climate change in the western Canadian boreal plain. Ecohydrology 9:899–908.

Schneider, R. R., A. Hamann, D. Farr, X. Wang, and S. Boutin. 2009. Potential effects of climate change on ecosystem distribution in Alberta. Canadian Journal of Forest Research 39:1001–1010.

Schneider, R. J., B. Stelfox, S. Boutin, and S. Wasel. 2003. Managing the cumulative impacts of land uses in the Western Canadian Sedimentary Basin: a modeling approach. Conservation Ecology 7:8.

Seidl, R., et al. 2017. Forest disturbances under climate change. Nature Climate Change 7:395–402.

Soja, A. J., et al. 2007. Climate-induced boreal forest change: predictions versus current observations. Global and Planetary Change 56:274–296.

Stephens, S. L., J. K. Agee, P. Z. Fulé, M. P. North, W. H. Romme, T. W. Swetnam, and M. G. Turner. 2013. Managing forests and fire in changing climates. Science 342:41–42.

Stocks, B. J., et al. 2002. Large forest fires in Canada, 1959–1997. Journal of Geophysical Research: Atmospheres 107:FFR 5-1–FFR 5-12.

Stralberg, D., S. M. Matsuoka, A. Hamann, E. M. Bayne, P. Sólymos, F. K. A. Schmiegelow, X. Wang, S. G. Cumming, and S. J. Song. 2015. Projecting boreal bird responses to climate change: The signal exceeds the noise. Ecological Applications 25:52–69.

Strong, W. L., and L. V. Hills. 2003. Post-Hypsithermal plant disjunctions in western Alberta, Canada. Journal of Biogeography 30:419–430.

Svenning, J.-C., and B. Sandel. 2013. Disequilibrium vegetation dynamics under future climate change. American Journal of Botany 100:1266–1286.

Taylor, K. E., R. J. Stouffer, and G. A. Meehl. 2012. An overview of CMIP5 and the experiment design. Bulletin of the American Meteorological Society 93:485–498.

Terrier, A., M. P. Girardin, C. Périé, P. Legendre, and Y. Bergeron. 2012. Potential changes in forest composition could reduce impacts of climate change on boreal wildfires. Ecological Applications 23:21–35.

Thompson, C., C. A. Mendoza, and K. J. Devito. 2017*a*. Potential influence of climate change on ecosystems within the Boreal Plains of Alberta. Hydrological Processes 31:2110–2124.

Thompson, D. K., M. A. Parisien, J. Morin, K. Millard, C. P. S. Larsen, and B. N. Simpson. 2017*b*. Fuel accumulation in a high-frequency boreal wildfire regime: from wetland to upland. Canadian Journal of Forest Research 47:957–964.

Turetsky, M. R., B. Benscoter, S. Page, G. Rein, G. R. van der Werf, and A. Watts. 2015. Global vulnerability of peatlands to fire and carbon loss. Nature Geoscience 8:11–14.

Tymstra, C., R. Bryce, B. Wotton, and O. Armitage. 2010. Development and structure of Prometheus: the Canadian wildland fire growth simulation model. Information Report NOR-X-417. Natural Resources Canada, Canadian Forest Service, Northern Forestry Centre, Edmonton, Alberta, Canada. https://cfs.nrcan.gc.ca/publications?id=31775

Tymstra, C., M. D. Flannigan, O. B. Armitage, and K. Logan. 2007. Impact of climate change on area burned in Alberta's boreal forest. International Journal of Wildland Fire 16:153–160.

Tymstra, C., D. Wang, and M.-P. Rogeau. 2005. Alberta wildfire regime analysis. Alberta Sustainable Resource Development, Forest Protection Division Wildfire Science and Technology Report PFFC-01-05, Edmonton, Alberta, Canada. https://archive.org/details/albertawildfirer00tyms_0

Van Wagner, C. E. 1969. A simple fire-growth model. Forestry Chronicle 45:103–104.

Van Wagner, C. E. 1987. Development and Structure of the Canadian Forest Fire Weather Index System. Forestry Technical Report 35. Canadian Forest Service, Ottawa, Ontario, Canada. https://cfs.nrcan.gc.ca/publications?id=19927

Veblen, T. T., T. Kitzberger, and J. Donnegan. 2000. Climatic and human influences on fire regimes in ponderosa pine forests in the Colorado front range. Ecological Applications 10:1178–1195.

Veraverbeke, S., B. M. Rogers, M. L. Goulden, R. R. Jandt, C. E. Miller, E. B. Wiggins, and J. T. Randerson. 2017. Lightning as a major driver of recent large fire years in North American boreal forests. Nature Climate Change 7:529–534.

Vitt, D. H., L. A. Halsey, and S. C. Zoltai. 2000. The changing landscape of Canada's western boreal forest: the current dynamics of permafrost. Canadian Journal of Forest Research 30:283–287.

Waddington, J. M., P. J. Morris, N. Kettridge, G. Granath, D. K. Thompson, and P. A. Moore. 2015. Hydrological feedbacks in northern peatlands. Ecohydrology 8:113–127.

Wang, X., M.-A. Parisien, M. D. Flannigan, S. A. Parks, K. R. Anderson, J. M. Little, and S. W. Taylor. 2014. The potential and realized spread of wildfires across Canada. Global Change Biology 20:2518–2530.

Wang, X., M.-A. Parisien, S. W. Taylor, J.-N. Candau, D. Stralberg, G. A. Marshall, J. M. Little, and M. D. Flannigan. 2017. Projected changes in daily fire spread across Canada over the next century. Environmental Research Letters 12:025005.

Wang, X., M.-A. Parisien, S. W. Taylor, D. D. B. Perrakis, J. Little, and M. D. Flannigan. 2016. Future burn probability in south-central British Columbia. International Journal of Wildland Fire 25:200–212.

Wang, X., D. K. Thompson, G. A. Marshall, C. Tymstra, R. Carr, and M. D. Flannigan. 2015. Increasing frequency of extreme fire weather in Canada with climate change. Climatic Change 130:573–586.

Watson, J. E. M., T. Iwamura, and N. Butt. 2013. Mapping vulnerability and conservation adaptation strategies under climate change. Nature Climate Change 3:989–994.

Whitman, E., E. Batllori, M.-A. Parisien, C. Miller, J. D. Coop, M. A. Krawchuk, G. W. Chong, and S. L. Haire. 2015. The climate space of fire regimes in north-western North America. Journal of Biogeography 42:1736–1749.

Whitman, E., M.-A. Parisien, D. K. Thompson, R. J. Hall, R. S. Skakun, and M. D. Flannigan. 2018. Variability and drivers of burn severity in the northwestern Canadian boreal forest. Ecosphere 9: e02128.

Williams, A. P., and J. T. Abatzoglou. 2016. Recent advances and remaining uncertainties in resolving past and future climate effects on global fire activity. Current Climate Change Reports 2:1–14.

Wotton, B. M., and M. D. Flannigan. 1993. Length of the fire season in a changing climate. Forestry Chronicle 69:187–192.

Wotton, B. M., C. A. Nock, and M. D. Flannigan. 2010. Forest fire occurrence and climate change in

Canada. International Journal of Wildland Fire 19:253–271.

Wu, D., X. Zhao, S. Liang, T. Zhou, K. Huang, B. Tang, and W. Zhao. 2015. Time-lag effects of global vegetation responses to climate change. Global Change Biology 21:3520–3531.

Zhang, J., S. Huang, and F. He. 2015. Half-century evidence from western Canada shows forest dynamics are primarily driven by competition followed by climate. Proceedings of the National Academy of Sciences of the United States of America 112: 4009–4014.

Supporting Information

Additional Supporting Information may be found online at: http://onlinelibrary.wiley.com/doi/10.1002/ecs2.2156/full

Ecosphere

Wildfire-mediated vegetation change in boreal forests of Alberta, Canada

Diana Stralberg, Xianli Wang, Marc-André Parisien, François-Nicolas Robinne, Péter Solymos, C. Lisa Mahon, Scott E. Nielsen, and Erin M. Bayne

Appendix 1

Ecosite and vegetation models

Ecosite and Vegetation Data

Hierarchical ecosite and vegetation types were based on the ecological land classification system of Alberta (Archibald et al. 1996, Beckingham and Archibald 1996) (Table S1). We omitted the natural subregion in the hierarchy to ensure that future vegetation was constrained by current soil moisture/nutrient status (i.e., ecosite) and climate, rather than arbitrary natural subregion boundaries, which will change with climate. We defined ecosite type as the (categorical) soil moisture and nutrient conditions of a site. We defined vegetation type (referred to as ecosite phase in the Alberta classification) as the combination of understory and overstory species found within a given ecosite type. In a climate-change context, the moisture component of our ecosite types should be considered relative to other ecosite types in the same climate zone. For example, mesic sites can be found throughout the province, but contain different vegetation depending on local climate conditions (including soil moisture): generally grassland in the prairie region, and aspen or white spruce in the boreal region.

Table S1. Ecosite and vegetation types considered. FBP = Canadian Forest Fire Behavior Prediction System fuel type for input to Burn-P3. O = grass fuel; D = deciduous fuel; M = boreal mixedwood fuel; C = conifer fuel. Codes with * were patched in post-hoc based on remotely sensed 2000 landcover (Pan et al. 2014).

Code	Ecosite	Vegetation Description	FBP	Cover Type	Upland	Forest
1	PX	Poor-Xeric Grassland	O-1	Grassland	1	0
2	PX	Poor-Xeric Jack Pine	C-1	Conifer	1	1
3	PM	Poor-Mesic Grassland	O-1	Grassland	1	0
4	PM	Poor-Mesic Pine	C-3	Conifer	1	1
5	PM	Poor-Mesic Black Spruce	C-2	Conifer	1	1
6	PG	Poor-Hygric Black Spruce	C-2	Conifer	0	1
7	PD	Poor-Hydric Black Spruce / Larch	C-1	Conifer	0	1
8	PD	Poor-Hydric Shrub	O-1	Shrub	0	0
9	MX	Medium-Xeric Grassland	O-1	Grassland	1	0
10	MX	Medium-Xeric Aspen Mix	M-1/2	Mixedwood	1	1
11	MX	Medium-Xeric Pine	C-1	Conifer	1	1
12	MX	Medium-Xeric Spruce	C-1	Conifer	1	1
13	MM	Medium-Mesic Grassland	O-1	Grassland	1	0
14	MM	Medium-Mesic Aspen	D-1/2	Deciduous	1	1
50	MM	Medium-Mesic Boreal Aspen	M-1/2	Mixedwood	1	1
15	MM	Medium-Mesic Aspen Mix	M-1/2	Mixedwood	1	1
16	MM	Medium-Mesic Pine	C-3	Conifer	1	1
17	MM	Medium-Mesic Pine Mix	C-3	Conifer	1	1
18	MM	Medium-Mesic White Spruce	C-2	Conifer	1	1
19	MG	Medium-Hygric Grassland	O-1	Grassland	0	0
20	MG	Medium-Hygric Poplar Mix	M-1/2	Deciduous	0	1
21	MG	Medium-Hygric Spruce Mix	C-2	Conifer	0	1
22	MG	Medium-Hygric Black Spruce Mix	C-2	Conifer	0	1
25	MD	Medium-Hydric Shrub Fen	O-1	Shrub	0	0
26	MD	Medium-Hydric Black Spruce Fen	O-1	Conifer	0	1
27	RM	Rich-Mesic Grassland	O-1	Grassland	1	0
28	RG	Rich-Hygric Shrubland	O-1	Shrub	0	0
29	RG	Rich-Hygric Poplar	D-1/2	Deciduous	0	1
30	RG	Rich-Hygric Lodgepole Pine	C-3	Conifer	0	1

Code	Ecosite	Vegetation Description	FBP	Cover Type	Upland	Forest
31	RG	Rich-Hygric Spruce	C-2	Conifer	0	1
32	RD	Rich-Hydric Grass Fen	O-1	Grassland	0	0
33	RD	Rich-Hydric Shrub Fen	O-1	Shrub	0	0
34	RD	Rich-Hydric Black Spruce	O-1	Conifer	0	1
35	SD	Marsh	nonfuel	Grassland	0	0
39*	OW	Open Water	nonfuel	None	0	0
41*	AG	Agriculture	nonfuel	None	0	0
42*	UR	Urban	nonfuel	None	0	0
43*	NF	Other Non-Fuel	nonfuel	None	0	0

To avoid propagating vegetation mapping errors, we used ground-based vegetation datasets rather than relying on remotely sensed data products to develop ecosite and vegetation models. We primarily used a terrestrial vegetation ("site capability") dataset from the Alberta Biodiversity Monitoring Institute (ABMI, http://www.abmi.ca/home/data-analytics) consisting of pre-determined sites arranged in a regular grid of 1,656 sites (not all sampled at the time of analysis) at 20-km intervals across Alberta, each consisting of a 3 × 3 sampling grid with adjacent points separated by 300 m (Boutin et al. 2009, Burton et al. 2014). ABMI's site capability classification is a generalized eco-type classification, modified from Beckingham and Archibald's (1996) ecological land classification system, and assessed in the field based on dominant vegetation within a 150-m radius around each survey point (details in Alberta Biodiversity Monitoring Institute 2014). We used the primary moisture and nutrient category (ecosite type) and tree species modifier (vegetation type).

A total of 5,369 points were available for analysis after we excluded highly developed sites without ecosite classifications, and added additional "off-grid" ABMI sites that were not part of the systematic sampling design. To improve model power, we also used generalized ecosite and vegetation classifications based on the ABMI protocol from a dataset collected by Environment Canada in the oil sands monitoring region (Mahon et al. 2016) (n = 3,776), as well as a University of Alberta dataset focused on boreal hill systems (S. Nielsen and E.M. Bayne unpubl.) (n = 115). We also added ecosite types from the georeferenced portion of the Alberta Government's Ecological Site Information System (ESIS) database (n = 820), which is derived from an intensive soil sampling protocol (https://open.alberta.ca/publications/5902534) for a total of 10,080 unique point locations used to develop ecosite models (Figure S1-1). Non-ESIS sites were classified in the field

between 2003 and 2014. ESIS sites were field-classified between 1992 and 1996. Although the site classifications spanned a 22-year period, our assumption was that moisture and nutrient category would remain constant during this period (as well as across the century-scale time period of our study).

We used the same dataset for the vegetation models, except for the ESIS dataset, which was not readily converted to classes consistent with the ABMI framework. Given the large ground-based sample available (n = 9,260), we chose to use this consistent, field-derived dataset even though it may result in greater apparent uncertainty in less well-sampled areas compared to remotely sensed landcover products.

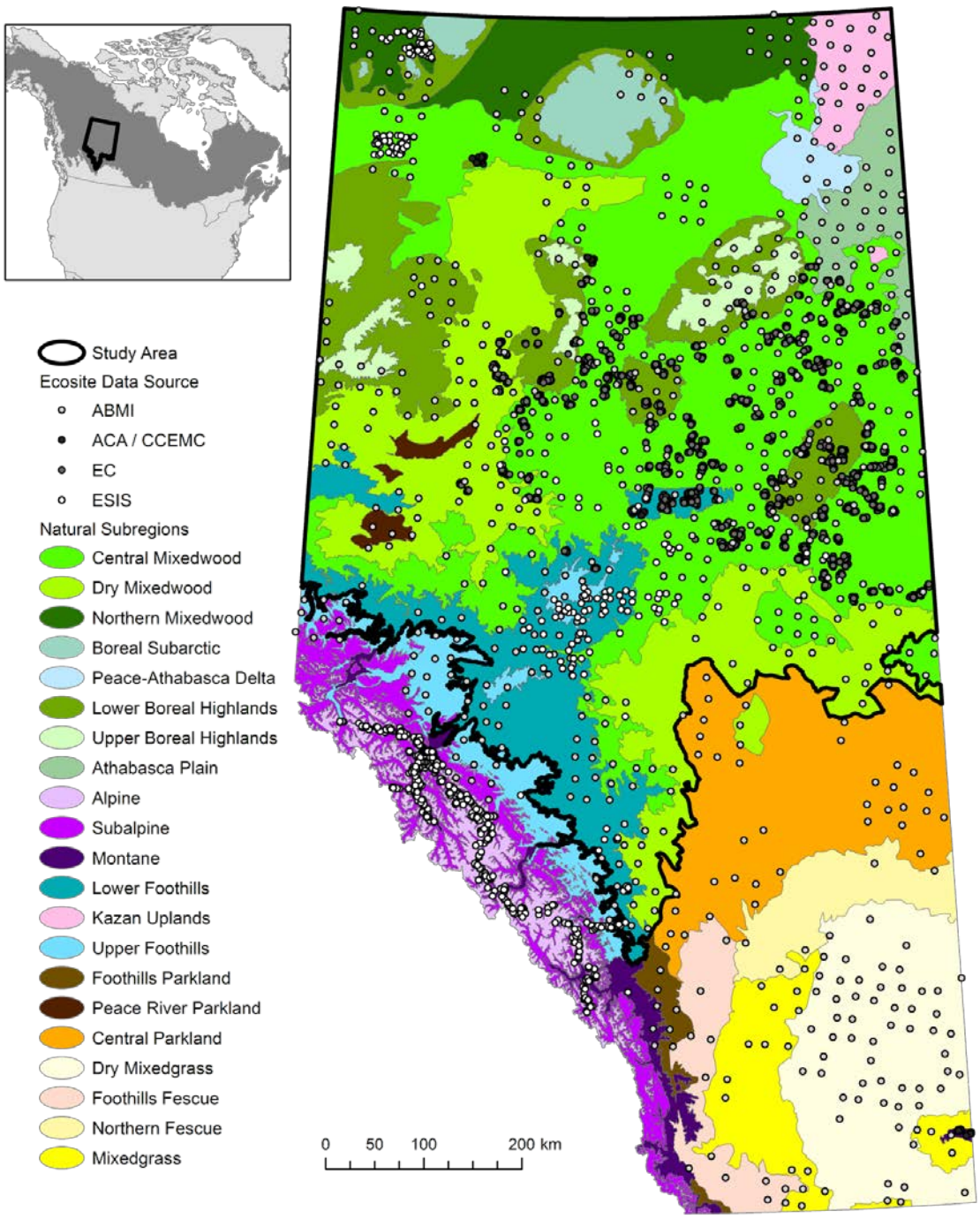

Figure S1. Study area and data locations with data source / project funding information. ABMI = Alberta Biodiversity Monitoring Institute; ACA = Alberta Conservation Association; CCEMC = Climate Change Emissions Management Corporation; EC = Environment Canada; ESIS = Ecological Site Information System.

Climate and Terrain Data

The climate, terrain, geology, and wetland variables used as inputs to ecosite and vegetation models are listed in Table S2. Terrain metrics were derived at 100-m raster resolution (S. Nielsen, University of Alberta, species.abmi.ca) and included indices of topographic ruggedness at various scales (VRM, vector ruggedness measure) (Sappington et al. 2007), slope, solar insolation, and terrain wetness (CTI, compound topographic index) (Gessler et al. 1995). Wetland classes were based on the Alberta merged wetland inventory derived from compiled vector polygon GIS layers with a minimum mapping unit of 0.09 ha (AESRD 2014), supplemented by a vegetation map for the Wood Buffalo National Park (Jensen 2003), which is not included in the provincial wetland inventory. Surficial geology was based on the surficial geology map of Alberta (map 601), which was derived from vector maps with source scales ranging from 1:50,000 to 1:1,000,000, compiled by the Alberta Geological Survey (2013).

Interpolated climate data for the 1961-1990 normal period based on the parameter-elevation regressions on independent slopes model (PRISM) (Daly et al. 2008) were obtained from Climate WNA at a 500-m resolution (Hamann et al. 2013). We used derived bioclimatic variables relevant to vegetation distributions (Table S2). To represent potential future climates for three consecutive 30-year periods (2011–2040, 2041–2070, and 2071–2100), we used projections from the Coupled Model Intercomparison Project, Phase 5 (CMIP5, Taylor et al. 2012): CanESM2 (Chylek et al. 2011), CESM1-CAM5 (Hurrell et al. 2013), and HadGEM2-ES (Jones et al. 2011).

Table S2. Climate, terrain, geology, and wetland variables included in random forest models for ecosite and vegetation. Variable importance values according to mean decrease in prediction accuracy (higher values = higher importance).

Variable	Definition	Ecosite	Vegetation
ahm	annual heat:moisture ratio	89.73	72.89
shm	summer heat:moisture ratio	93.74	70.00
ddlt18	degree days < 18 °C	98.79	73.26
msp	mean summer (May-Sep) precipitation	84.26	69.57
td	temperature difference (summer – winter)	86.39	69.10
emt	extreme minimum temperature	88.66	63.50
slpasp	slope / aspect solar radiation index	47.39	54.85
tpi2km	topographic position index (2-km radius)	65.25	57.42
vrm11x11	vector ruggedness measure (11 x 11 cells)	49.93	58.07
cti	compound topographic index (wetness)	38.10	36.81
slope	slope	49.61	-
landform	landform	31.17	-
geol_surf	surficial geology (parent material)	94.22	-
wetlands	wetland type	107.14	-
ecosite	ecosite type	-	182.43

Ecosite and Vegetation Models

Although our approach was similar to that of predictive ecosystem mapping efforts used for resource inventory purposes (Franklin 1995, MacMillan et al. 2007), our climate-change focus meant that we built our model using a larger spatial extent and a coarser spatial resolution than traditional modelling efforts that emphasize high site-level accuracy over model generality. Because we used climate variables as a proxy for traditionally-used ecoregion boundaries, our baseline spatial predicted values should be interpreted with caution in data deficient areas of the province, primarily in the north and in the west (see Figure S1-1). Our focus was on boreal Alberta, but we used data from throughout the province, including prairie and Rocky mountain regions, to capture the climate conditions that are likely to move northward into the boreal region in the future (Schneider et al. 2009), and to model climate-vegetation relationships across a wider range of conditions, respectively.

As a basis for identifying topo-edaphic constraints on future projections of vegetation types, we first modelled ecosite as a function of geology, climate, terrain, and mapped wetland class sampled at 100-m grid cell resolution (n = 10,080). The influence of these variables can be viewed in a hierarchical manner. Regionally, surficial geology provides the parent material from which soils are created, and influences nutrient availability; climate determines rates of evapotranspiration and available moisture. At the landscape level, terrain features redistribute solar energy and determine the flow of water and resulting moisture characteristics. Thus, we presumed that terrain, climate, and geology could be used to predict moisture and nutrient conditions at an accuracy level suitable for province-wide analysis. We also included the Alberta merged wetland inventory as a covariate to help improve predictions of current wetland ecosites (held static into the future), although accuracy varies by data source across the province.

We used a random forest (Breiman 2001) classification-tree approach to develop predictive models for 12 ecosite types, 5 of which were considered uplands (Table S1). Random forest is a powerful ensemble approach based on sophisticated bootstrap sampling and subsequent averaging of the data. It is widely used in vegetation mapping (Evans and Cushman 2009) and species distribution modelling (Iverson et al. 2004, Rehfeldt et al. 2006, Oppel and Huettmann 2010) due to its high predictive performance (Elith et al. 2006, Prasad et al. 2006, Syphard and Franklin 2009). Models were constructed in 64-bit R v. 3.1.3 (R Core Team 2014) using the 'randomForest' package (Liaw 2015). Since random forest is an ensemble model approach, performance was assessed according to out-of-bag (OOB) classification accuracy.

For prediction purposes (vs. model-building), we used 500-m resolution raster layers, even for variables originally sampled at a 100-m resolution, to improve speed and reduce storage requirements, given the boreal scale of the analysis and the focus on regional and landscape-level estimation rather than prediction at individual grid cells.

Because we assumed ecosites would not change state over the next century, we used predicted ecosite types, along with climate and terrain variables, as inputs to random forest models for 32 vegetation types (Table S1). The terrain variables were included again at this stage to allow for terrain-driven variability within a given ecosite. For example, within the extensive medium-mesic ecosite, the probability of white spruce vs. aspen growth may be related to site exposure (e.g., landform and aspect), as well as temperature and precipitation.

In contrast, geology and wetlands were considered first-order classifiers better suited to differentiating among ecosites.

Model Results and Accuracy

Random forest models for 12 ecosite classes had an out-of-bag (OOB) error rate of 38% (accuracy = 62%) (Table S3). The lowest classification error (11%) was for the medium mesic (MM) upland ecosite type, which was predicted to comprise 50% of the province, including urban and agricultural areas. The highest classification error (100%) was for the marsh (VG) wetland ecosite type, which had only 26 records and could not be differentiated from other wetland ecosite types. The large majority of misclassified records were correctly classified by either moisture or nutrient status. The pooled OOB error rate for upland vs. wetland classes was 20%. For specific moisture class it was 28% and for nutrient class it was 27%. The most important explanatory variable in terms of decrease in accuracy was the wetland class variable, followed by growing degree days less than 18° C, surficial geology, summer heat:moisture ratio, and annual heat:moisture ratio (Table S2). Predicted vegetation classes are shown in Figure S1-3.

Random forest models for 40 vegetation types had an OOB error rate of 19% (accuracy = 81%), with error rates for individual vegetation types ranging from 0% (medium-mesic grassland, rich-mesic grassland, poor-hygric black spruce, poor-hydric black spruce/larch) to 71% (poor-hydric shrub) (Table S4). Combining vegetation types by FBP System fuel type, the average prediction accuracy was 89% (Table S5). The most important explanatory variable by far in terms of decrease in accuracy was the ecosite class variable, followed by growing degree days less than 18° C, annual heat:moisture ratio, and summer heat:moisture ratio (Table S2). Predicted vegetation classes are shown in Figure S3.

Table S3. Confusion matrix for ecosite classification model. Upland (X = xeric, M = mesic) grouped separately from lowland (G = hygric, D = hydric) moisture classes. Nutrient class definitions: P = poor, M = medium, R = rich. See S1-1 for full ecosite code definitions. Upland classes in bold.

	PX	**PM**	**MX**	**MM**	**RM**	MG	MD	PG	PD	RG	RD	SD	Class Error
PX	**224**	**54**	**5**	**128**	**0**	1	4	0	5	1	6	0	0.48
PM	**39**	**520**	**5**	**402**	**1**	11	28	22	63	7	22	0	0.54
MX	**13**	**16**	**90**	**29**	**0**	10	6	0	7	1	2	0	0.61
MM	**39**	**127**	**12**	**3555**	**0**	69	26	17	43	83	31	0	0.11
RM	**0**	**0**	**0**	**12**	**27**	0	0	0	0	0	0	0	0.31
MG	2	31	10	360	1	263	17	9	11	19	40	0	0.66
MD	7	39	0	80	0	11	235	36	58	2	85	0	0.58
PG	1	25	0	94	0	6	60	172	40	6	26	1	0.61
PD	9	73	1	125	0	10	33	33	368	7	34	0	0.51
RG	1	11	0	481	0	16	3	6	11	308	20	0	0.64
RD	9	36	1	102	0	28	72	20	45	11	337	0	0.49
SD	0	0	0	5	0	0	3	5	1	1	11	1	1.00

Table S4. Confusion matrix for random forest vegetation predictions.

Code	Vegetation Classification	Ecosite	Class Error	1	2	3
1	Poor-Xeric Grassland	PX	0.07	40	0	1
2	Poor-Xeric Jack Pine	PX	0.01	0	273	0
3	Poor-Mesic Grassland	PM	0.32	0	0	73
4	Poor-Mesic Pine	PM	0.25	0	0	1
5	Poor-Mesic Black Spruce	PM	0.07	0	0	3
6	Poor-Hygric Black Spruce	PG	0.00	0	0	0
7	Poor-Hydric Black Spruce / Larch	PD	0.00	0	0	0
8	Poor-Hydric Shrub	PD	0.33	0	0	0
9	Medium-Xeric Grassland	MX	0.06	0	0	1
10	Medium-Xeric Aspen Mix	MX	0.24	0	0	0
11	Medium-Xeric Pine	MX	0.30	0	1	0
12	Medium-Xeric Spruce	MX	0.23	0	1	0
13	Medium-Mesic Grassland	MM	0.00	0	0	0
14	Medium-Mesic Aspen	MM	0.15	0	0	0
50	Medium-Mesic Aspen Boreal Mixedwood	MM	0.12	0	0	0
15	Medium-Mesic Aspen Mix	MM	0.53	0	0	0
16	Medium-Mesic Pine	MM	0.22	0	0	0
17	Medium-Mesic Pine Mix	MM	0.42	0	0	0
18	Medium-Mesic White Spruce	MM	0.57	0	0	0
19	Medium-Hygric Grassland	MG	0.01	0	0	0
20	Medium-Hygric Poplar Mix	MG	0.11	0	0	0
21	Medium-Hygric Spruce Mix	MG	0.34	0	0	1
22	Medium-Hygric Black Spruce Mix	MG	0.37	0	0	0
25	Medium-Hydric Shrub (Poor Fen)	MD	0.71	0	0	0
26	Medium-Hydric Black Spruce Fen (Poor Fen)	MD	0.04	0	0	1
27	Rich-Mesic Grassland	RM	0.00	0	0	0
28	Rich-Hygric Shrubland	RG	0.30	1	0	0
29	Rich-Hygric Poplar	RG	0.03	0	0	0
30	Rich-Hygric Lodgepole Pine	RG	0.38	0	0	0
31	Rich-Hygric Spruce	RG	0.38	0	0	0

32	Rich-Hydric Grass Fen	RD	0.45	1	0	0
33	Rich-Hydric Shrub Fen	RD	0.26	0	0	0
34	Rich-Hydric Black Spruce	RD	0.19	0	0	0
37	Very Rich-Hydric Marsh	VD	0.20	0	0	0

Code	4	5	6	7	8	9	10	11	12	13	14	50	15	16
1	0	0	0	0	0	0	0	0	0	0	0	0	0	0
2	1	0	0	0	0	0	1	0	0	0	0	0	0	0
3	14	16	0	0	0	0	1	0	1	0	0	0	0	0
4	155	52	0	0	0	0	0	0	0	0	0	0	0	0
5	23	340	0	0	0	0	1	0	0	0	0	0	0	0
6	0	0	33	0	0	0	0	0	0	0	0	0	0	0
7	0	0	0	459	2	0	0	0	0	0	0	0	0	0
8	0	0	0	11	22	0	0	0	0	0	0	0	0	0
9	0	0	0	0	0	44	0	1	0	0	0	0	0	0
10	0	1	0	0	0	0	47	10	1	0	0	0	0	0
11	0	3	0	0	0	0	6	45	3	0	0	0	0	0
12	0	0	0	0	0	0	4	4	30	0	0	0	0	0
13	0	0	0	0	0	0	0	0	0	325	0	1	0	0
14	0	0	0	0	0	0	0	0	0	1	181	4	18	0
50	0	0	0	0	0	0	0	0	0	1	1	913	89	2
15	0	0	0	0	0	0	0	0	0	0	22	204	239	8
16	0	0	0	0	0	0	0	0	0	0	0	9	7	105
17	0	0	0	0	0	0	0	0	0	0	1	67	20	9
18	0	0	0	0	0	0	0	0	0	0	9	63	48	10
19	0	0	0	0	0	0	0	0	0	0	0	0	0	0
20	0	0	0	0	0	1	0	0	0	0	0	0	0	0
21	0	1	0	0	0	0	0	0	1	0	0	0	0	0
22	0	1	1	0	0	0	0	1	0	0	0	0	0	0
25	0	0	0	0	0	0	0	0	0	0	0	0	0	0
26	0	1	0	0	0	0	0	1	0	0	0	0	0	0
27	0	0	0	0	0	0	0	0	0	0	0	0	0	0
28	0	0	0	0	0	0	0	0	0	0	0	0	0	0
29	0	0	0	0	0	0	0	0	0	0	0	0	0	0
30	0	0	0	0	0	0	0	0	0	0	0	0	0	0
31	0	0	0	0	0	0	0	0	0	0	0	0	0	0
32	0	0	0	0	0	1	0	0	0	0	0	0	0	0
33	1	0	0	1	0	0	0	0	0	0	0	0	0	0
34	1	0	0	1	0	0	1	0	0	0	0	0	0	0
37	0	0	0	0	0	0	0	0	0	0	0	0	1	0

Code	17	18	19	20	21	22	25	26	27	28	29	30	31	32
1	0	0	0	0	0	0	0	0	0	1	0	0	0	0
2	0	0	0	0	0	0	0	0	0	0	0	0	0	0
3	0	0	0	0	1	0	0	0	1	0	0	0	0	0
4	0	0	0	0	0	0	0	0	0	0	0	0	0	0
5	0	0	0	0	0	0	0	0	0	0	0	0	0	0
6	0	0	0	0	0	0	0	0	0	0	0	0	0	0
7	0	0	0	0	0	0	0	0	0	0	0	0	0	0
8	0	0	0	0	0	0	0	0	0	0	0	0	0	0
9	0	0	1	0	0	0	0	0	0	0	0	0	0	0
10	0	0	0	2	0	0	0	1	0	0	0	0	0	0
11	0	0	0	4	0	0	1	1	0	0	0	0	0	0
12	0	0	0	0	0	0	0	0	0	0	0	0	0	0
13	0	0	0	0	0	0	0	0	0	0	0	0	0	0
14	0	8	0	0	0	0	0	0	0	0	0	0	0	0
50	16	20	0	0	0	0	0	0	0	0	0	0	0	0
15	12	28	0	0	0	0	0	0	0	0	0	0	0	0
16	8	6	0	0	0	0	0	0	0	0	0	0	0	0
17	143	8	0	0	0	0	0	0	0	0	0	0	0	0
18	7	104	0	0	0	0	0	0	0	0	0	0	0	0
19	0	0	122	0	0	0	0	0	1	0	0	0	0	0
20	0	0	0	232	18	9	0	0	0	0	0	0	0	0
21	0	1	1	31	85	4	0	0	0	0	0	0	0	0
22	0	0	0	18	9	58	0	3	0	0	0	0	0	0
25	0	0	0	0	0	0	12	29	0	0	0	0	0	0
26	0	0	0	0	0	1	4	235	0	0	0	0	0	0
27	0	0	0	0	0	0	0	0	36	0	0	0	0	0
28	0	0	2	0	0	0	0	0	0	7	0	0	0	0
29	0	0	0	0	0	0	0	0	0	0	475	2	14	0
30	0	0	0	0	0	0	0	0	0	0	3	13	5	0
31	0	0	0	0	0	0	0	0	0	0	32	5	61	0
32	0	0	1	0	0	0	0	0	2	1	0	0	0	24
33	0	0	0	2	0	0	0	0	0	0	0	0	0	5
34	0	0	0	0	0	2	0	4	0	0	0	0	0	1
37	0	0	0	0	0	0	0	0	0	0	0	0	0	0

Code	33	34	37
1	1	0	0
2	0	0	0
3	0	0	0
4	0	0	0
5	0	0	0
6	0	0	0
7	0	0	0
8	0	0	0
9	0	0	0
10	0	0	0
11	0	0	0
12	0	0	0
13	0	0	0
14	0	0	0
50	0	0	0
15	0	0	0
16	0	0	0
17	0	0	0
18	0	0	0
19	0	0	0
20	0	0	0
21	1	2	0
22	0	1	0
25	0	0	0
26	1	0	0
27	0	0	0
28	0	0	0
29	0	0	0
30	0	0	0
31	0	0	0
32	10	4	0
33	143	41	0
34	33	183	0
37	0	0	4

Table S5**.** Confusion matrix for vegetation classification model, grouped by fuel type. See Table S1 for fuel code correspondence with vegetation types. C-1, C-2 and C-3 represent conifer fuels. D-1/2 is deciduous, M-1/2 is mixedwood, and O-1 is grassland. The only nonfuel vegetation type modelled was marsh (SD).

	C-1	C-2	C-3	D-1/2	M-1/2	O-1	Nonfuel	Class Error
C-1	817	3	0	0	12	15	0	0.04
C-2	5	702	72	16	75	19	0	0.21
C-3	0	46	431	2	38	12	0	0.19
D-1/2	0	41	6	665	25	0	0	0.10
M-1/2	12	156	102	19	1724	5	1	0.15
O-1	5	11	1	1	3	1422	0	0.01
Nonfuel	0	0	0	0	0	0	4	0.00

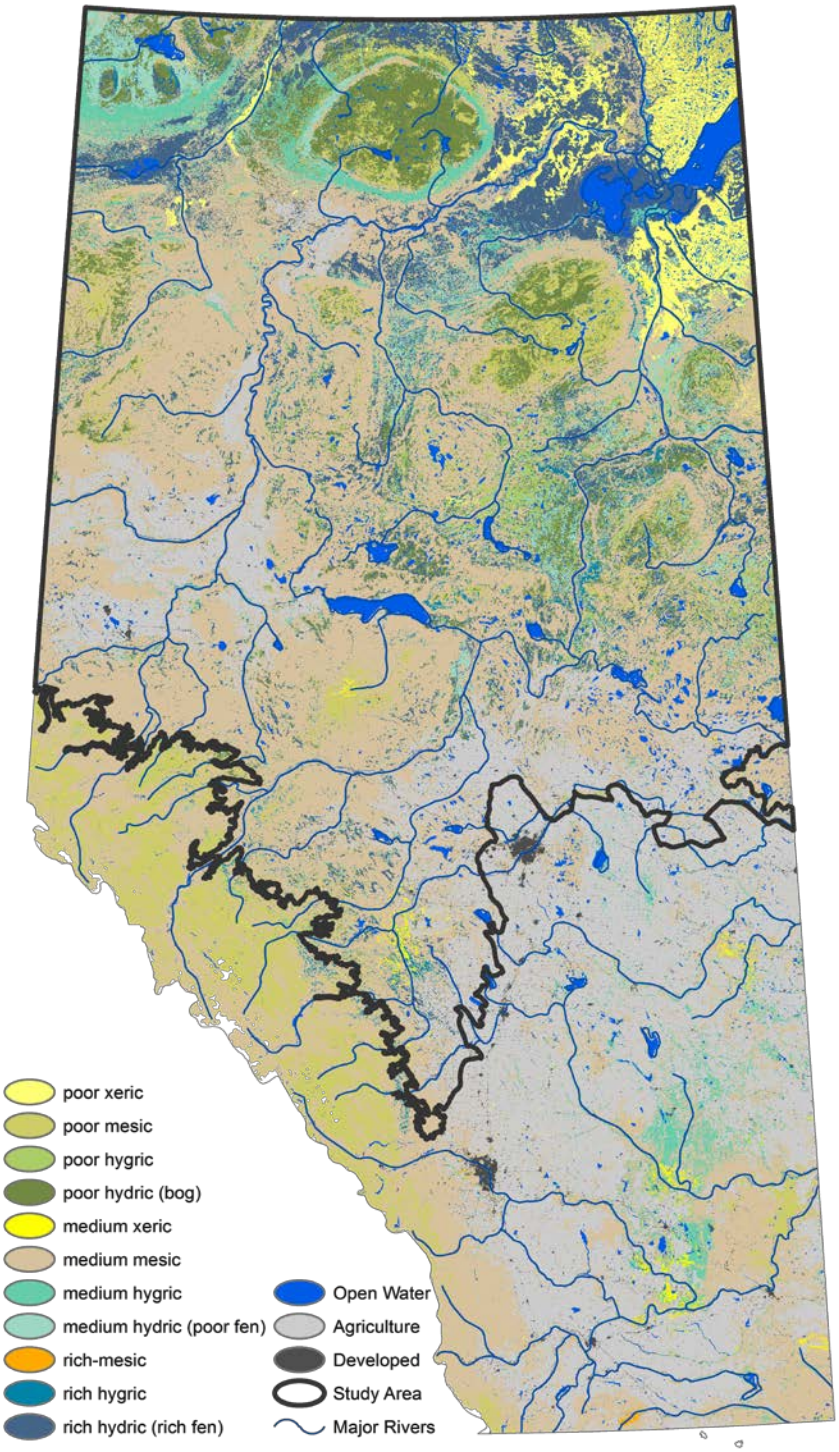

Figure S2. Predicted ecosite type (relative soil moisture/nutrient combination). Open water, agriculture, and developed areas are taken from ABMI's wall-to-wall landcover layer.

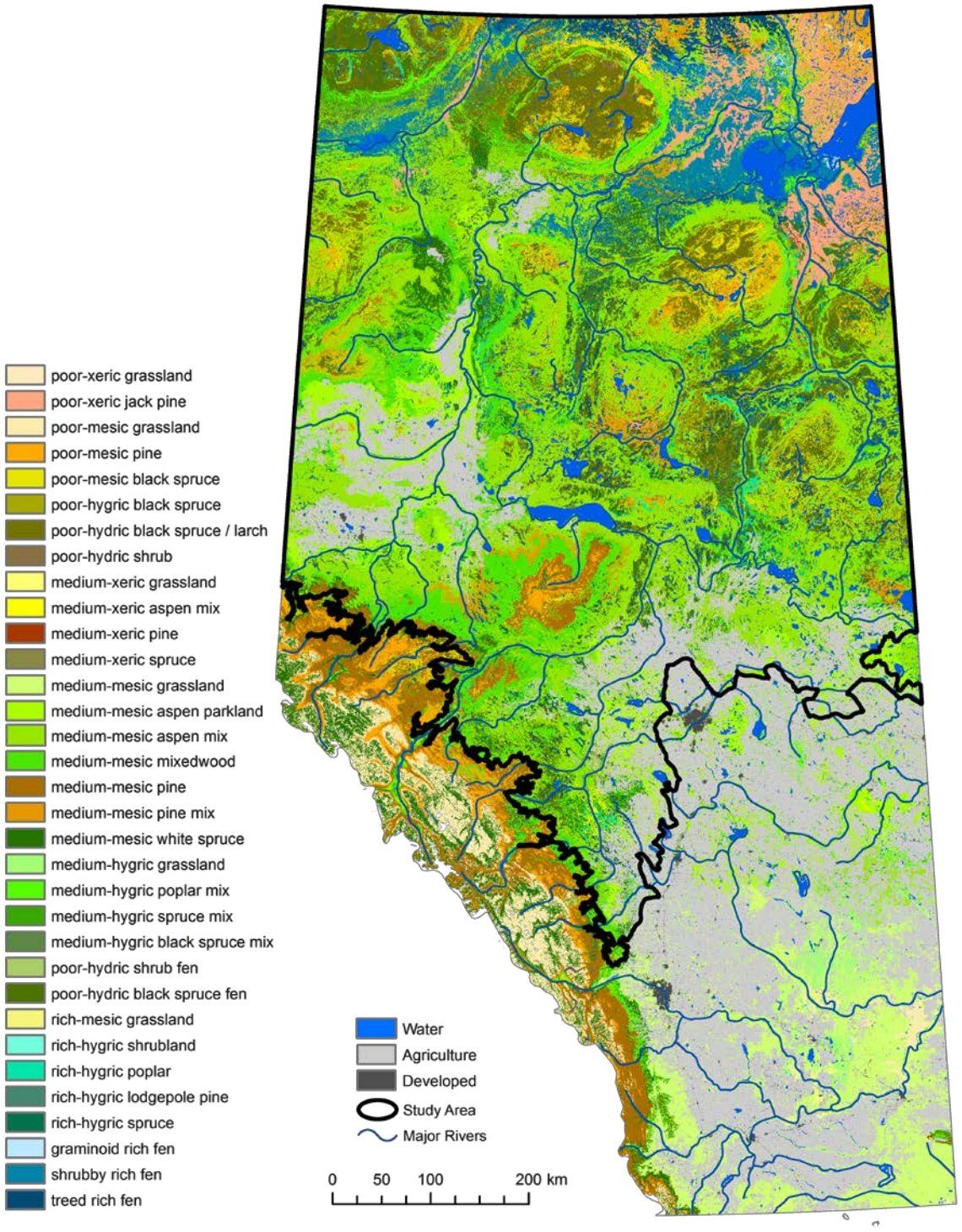

Figure S3. Predicted current vegetation type as a function of ecosite, terrain, and climate.

AESRD. 2014. Alberta Merged Wetland Inventory. Alberta Environment and Sustainable Resource Development. Edmonton, AB.
Alberta Biodiversity Monitoring Institute. 2014. Terrestrial field data collection protocols (abridged version) 2017-03-27. Alberta Biodiversity Monitoring Institute, Alberta, Canada. Report available at: http://abmi.ca.
Alberta Geological Survey. 2013. Surficial Geology Map of Alberta *in* A. G. Survey, editor., Edmonton, Alberta.
Archibald, J. H., G. D. Klappstein, and I. G. W. Corns. 1996. Field guide to ecosites of Southwestern Alberta. Natural Resources Canada, Canadian Forest Service, Edmonton, Alberta.
Beckingham, J. D., and J. H. Archibald. 1996. Field guide to ecosites of Northern Alberta. Natural Resources Canada, Canadian Forest Service, Edmonton, AB.
Boutin, S., D. L. Haughland, J. Schieck, J. Herbers, and E. Bayne. 2009. A new approach to forest biodiversity monitoring in Canada. Forest Ecology and Management 258, Supplement:S168-S175.
Breiman, L. 2001. Random Forests. Machine Learning 45:5-32.
Burton, A. C., D. Huggard, E. Bayne, J. Schieck, P. Sólymos, T. Muhly, D. Farr, and S. Boutin. 2014. A framework for adaptive monitoring of the cumulative effects of human footprint on biodiversity. Environmental Monitoring and Assessment:1-13.
Chylek, P., J. Li, M. K. Dubey, M. Wang, and G. Lesins. 2011. Observed and model simulated 20th century Arctic temperature variability: Canadian Earth System Model CanESM2. Atmos. Chem. Phys. Discuss. 2011:22893-22907.
Daly, C., M. Halbleib, J. I. Smith, W. P. Gibson, M. K. Doggett, G. H. Taylor, J. Curtis, and P. P. Pasteris. 2008. Physiographically sensitive mapping of climatological temperature and precipitation across the conterminous United States. International Journal of Climatology 28:2031-2064.
Elith, J., C. H. Graham, R. P. Anderson, M. Dudik, S. Ferrier, A. Guisan, R. J. Hijmans, F. Huettmann, J. R. Leathwick, A. Lehmann, J. Li, L. G. Lohmann, B. A. Loiselle, G. Manion, C. Moritz, M. Nakamura, Y. Nakazawa, J. McC. M. Overton, A. Townsend Peterson, S. J. Phillips, K. Richardson, R. Scachetti-Pereira, R. E. Schapire, J. Soberón, S. Williams, M. S. Wisz, and N. E. Zimmermann. 2006. Novel methods improve prediction of species' distributions from occurrence data. Ecography 29:129-151.
Evans, J., and S. Cushman. 2009. Gradient modeling of conifer species using random forests. Landscape Ecology 24:673-683.
Franklin, J. 1995. Predictive vegetation mapping: geographic modelling of biospatial patterns in relation to environmental gradients. Progress in Physical Geography 19:474-499.
Gessler, P. E., I. D. Moore, M. N.J., and R. P.J. 1995. Soil-landscape modeling and spatial prediction of soil attributes. International Journal of GIS 9:421-432.
Hamann, A., T. Wang, D. L. Spittlehouse, and T. Q. Murdock. 2013. A comprehensive, high-resolution database of historical and projected climate surfaces for western North America Bulletin of the American Meteorological Society 94:1307–1309.
Hurrell, J. W., M. M. Holland, P. R. Gent, S. Ghan, J. E. Kay, P. J. Kushner, J. F. Lamarque, W. G. Large, D. Lawrence, K. Lindsay, W. H. Lipscomb, M. C. Long, N. Mahowald, D. R. Marsh, R. B. Neale, P. Rasch, S. Vavrus, M. Vertenstein, D. Bader, W. D. Collins, J. J. Hack, J. Kiehl, and S. Marshall. 2013. The Community Earth System Model: A

Framework for Collaborative Research. Bulletin of the American Meteorological Society 94:1339-1360.
Iverson, L. R., M. W. Schwartz, and A. M. Prasad. 2004. How fast and far might tree species migrate in the eastern United States due to climate change? Global Ecology and Biogeography 13:209-219.
Jensen, O. 2003. Wood Buffalo National Park Vegetation Classification Final Report.
Jones, C. D., J. K. Hughes, N. Bellouin, S. C. Hardiman, G. S. Jones, J. Knight, S. Liddicoat, F. M. O'Connor, R. J. Andres, C. Bell, K. O. Boo, A. Bozzo, N. Butchart, P. Cadule, K. D. Corbin, M. Doutriaux-Boucher, P. Friedlingstein, J. Gornall, L. Gray, P. R. Halloran, G. Hurtt, W. J. Ingram, J. F. Lamarque, R. M. Law, M. Meinshausen, S. Osprey, E. J. Palin, L. Parsons Chini, T. Raddatz, M. G. Sanderson, A. A. Sellar, A. Schurer, P. Valdes, N. Wood, S. Woodward, M. Yoshioka, and M. Zerroukat. 2011. The HadGEM2-ES implementation of CMIP5 centennial simulations. Geoscientific Model Development 4:543-570.
Liaw, A. 2015. Package 'randomForest'. Available on-line at http://cran.r-project.org/web/packages/randomForest/index.html.
MacMillan, R. A., D. E. Moon, and R. A. Coupé. 2007. Automated predictive ecological mapping in a Forest Region of B.C., Canada, 2001–2005. Geoderma 140:353-373.
Mahon, C. L., G. H. Holloway, P. Solymos, S. G. Cumming, E. M. Bayne, F. K. A. Schmiegelow, and S. J. Song. 2016. Community structure and niche characteristics of upland and lowland western boreal birds at multiple spatial scales. Forest Ecology and Management 361:99-116.
Oppel, S., and F. Huettmann. 2010. Using a Random Forest Model and Public Data to Predict the Distribution of Prey for Marine Wildlife Management. Pages 151-163 *in* S. Cushman and F. Huettmann, editors. Spatial Complexity, Informatics, and Wildlife Conservation. Springer Japan.
Pan, D., J. Schieck, and S. F. Morrison. 2014. 2000 Alberta Backfilled Wall-to-Wall Land Cover Version 2.5 - Metadata. http://www.abmi.ca/home/publications/301-350/349.html.
Prasad, A. M., L. R. Iverson, and A. Liaw. 2006. Newer classification and regression tree techniques: bagging and random forests for ecological prediction. Ecosystems 9:181-199.
Rehfeldt, G. E., N. L. Crookston, M. V. Warwell, and J. S. Evans. 2006. Empirical analyses of plant-climate relationships for the western United States. International Journal of Plant Sciences 167:1123-1150.
Sappington, J. M., K. M. Longshore, and D. B. Thompson. 2007. Quantifying Landscape Ruggedness for Animal Habitat Analysis: A Case Study Using Bighorn Sheep in the Mojave Desert. The Journal of Wildlife Management 71:1419-1426.
Schneider, R. R., A. Hamann, D. Farr, X. Wang, and S. Boutin. 2009. Potential effects of climate change on ecosystem distribution in Alberta. Canadian Journal of Forest Research 39:1001-1010.
Syphard, A. D., and J. Franklin. 2009. Differences in spatial predictions among species distribution modeling methods vary with species traits and environmental predictors. Ecography 32:907-918.
Taylor, K. E., R. J. Stouffer, and G. A. Meehl. 2012. An Overview of CMIP5 and the Experiment Design. Bulletin of the American Meteorological Society 93:485-498.

Ecosphere

Wildfire-mediated vegetation change in boreal forests of Alberta, Canada

Diana Stralberg, Xianli Wang, Marc-André Parisien, François-Nicolas Robinne, Péter Solymos, C. Lisa Mahon, Scott E. Nielsen, and Erin M. Bayne

Appendix 2. Burn-P3 fire simulation settings

Table S1. Full list of parameters and inputs for Burn-P3 scenarios. The number of model iterations is specified per fuel iteration as needed (i.e., 300 model iterations x 10 fuel iterations).

ID	Time Period	Fuel Scenario	Fire Regime Scenario	GCM	Iterations	Fuel	Weather	Number of escaped fires	Spread day distribution
1	1980-2010	All equivalent	Constrained	N/A	3000	Baseline (1961-1990 climate)	1980-2010	Baseline (1981-2010 weather)	Baseline (1980-2010 weather)
2	2011-2040	All equivalent	Constrained	CanESM2	3000	Baseline (1961-1990 climate)	2011-2040	Baseline (1981-2010 weather)	Baseline (1980-2010 weather)
3	2011-2040	All equivalent	Constrained	CSIRO	3000	Baseline (1961-1990 climate)	2011-2040	Baseline (1981-2010 weather)	Baseline (1980-2010 weather)
4	2011-2040	All equivalent	Constrained	HadGEM2	3000	Baseline (1961-1990 climate)	2011-2040	Baseline (1981-2010 weather)	Baseline (1980-2010 weather)
5	2011-2040	All equivalent	Unconstrained	CanESM2	3000	Baseline (1961-1990 climate)	2011-2040	Unconstrained	Unconstrained
6	2011-2040	All equivalent	Unconstrained	HadGEM2	3000	Baseline (1961-1990 climate)	2011-2040	Unconstrained	Unconstrained
7	2011-2040	All equivalent	Unconstrained	CSIRO	3000	Baseline (1961-1990 climate)	2011-2040	Unconstrained	Unconstrained
8	2041-2070	Static fuels	Constrained	CanESM2	3000	Baseline (1961-1990 climate)	2041-2070	Baseline (1981-2010 weather)	Baseline (1980-2010 weather)
9	2071-2100	Static fuels	Constrained	CanESM2	3000	Baseline (1961-1990 climate)	2071-2100	Baseline (1981-2010 weather)	Baseline (1980-2010 weather)
10	2041-2070	Static fuels	Constrained	CSIRO	3000	Baseline (1961-1990 climate)	2041-2070	Baseline (1981-2010 weather)	Baseline (1980-2010 weather)

ID	Time Period	Fuel Scenario	Fire Regime Scenario	GCM	Iterations	Fuel	Weather	Number of escaped fires	Spread day distribution
11	2071-2100	Static fuels	Constrained	CSIRO	3000	Baseline (1961-1990 climate)	2071-2100	Baseline (1981-2010 weather)	Baseline (1980-2010 weather)
12	2041-2070	Static fuels	Constrained	HadGEM2	3000	Baseline (1961-1990 climate)	2041-2070	Baseline (1981-2010 weather)	Baseline (1980-2010 weather)
13	2071-2100	Static fuels	Constrained	HadGEM2	3000	Baseline (1961-1990 climate)	2071-2100	Baseline (1981-2010 weather)	Baseline (1980-2010 weather)
14	2041-2070	Static fuels	Unconstrained	CanESM2	3000	Baseline (1961-1990 climate)	2041-2070	Unconstrained	Unconstrained
15	2071-2100	Static fuels	Unconstrained	CanESM2	3000	Baseline (1961-1990 climate)	2071-2100	Unconstrained	Unconstrained
16	2041-2070	Static fuels	Unconstrained	CSIRO	3000	Baseline (1961-1990 climate)	2041-2070	Unconstrained	Unconstrained
17	2071-2100	Static fuels	Unconstrained	CSIRO	3000	Baseline (1961-1990 climate)	2071-2100	Unconstrained	Unconstrained
18	2041-2070	Static fuels	Unconstrained	HadGEM2	3000	Baseline (1961-1990 climate)	2041-2070	Unconstrained	Unconstrained
19	2071-2100	Static fuels	Unconstrained	HadGEM2	3000	Baseline (1961-1990 climate)	2071-2100	Unconstrained	Unconstrained
20	2041-2070	Climate-driven fuels	Constrained	CanESM2	3000	2011-2040 climate-based	2041-2070	Baseline (1981-2010 weather)	Baseline (1980-2010 weather)
21	2071-2100	Climate-driven fuels	Constrained	CanESM2	3000	2041-2070 climate-based	2071-2100	Baseline (1981-2010 weather)	Baseline (1980-2010 weather)

ID	Time Period	Fuel Scenario	Fire Regime Scenario	GCM	Iterations	Fuel	Weather	Number of escaped fires	Spread day distribution
22	2041-2070	Climate-driven fuels	Constrained	CSIRO	3000	2011-2040 climate-based	2041-2070	Baseline (1981-2010 weather)	Baseline (1980-2010 weather)
23	2071-2100	Climate-driven fuels	Constrained	CSIRO	3000	2041-2070 climate-based	2071-2100	Baseline (1981-2010 weather)	Baseline (1980-2010 weather)
24	2041-2070	Climate-driven fuels	Constrained	HadGEM2	3000	2011-2040 climate-based	2041-2070	Baseline (1981-2010 weather)	Baseline (1980-2010 weather)
25	2071-2100	Climate-driven fuels	Constrained	HadGEM2	3000	2041-2070 climate-based	2071-2100	Baseline (1981-2010 weather)	Baseline (1980-2010 weather)
26	2041-2070	Climate-driven fuels	Unconstrained	CanESM2	3000	2011-2040 fire-mediated	2041-2070	Unconstrained	Unconstrained
27	2071-2100	Climate-driven fuels	Unconstrained	CanESM2	3000	2041-2070 fire-mediated	2071-2100	Unconstrained	Unconstrained
28	2041-2070	Climate-driven fuels	Unconstrained	CSIRO	3000	2011-2040 fire-mediated	2041-2070	Unconstrained	Unconstrained
29	2071-2100	Climate-driven fuels	Unconstrained	CSIRO	3000	2041-2070 fire-mediated	2071-2100	Unconstrained	Unconstrained
30	2041-2070	Climate-driven fuels	Unconstrained	HadGEM2	3000	2011-2040 fire-mediated	2041-2070	Unconstrained	Unconstrained
31	2071-2100	Climate-driven fuels	Unconstrained	HadGEM2	3000	2041-2070 fire-mediated	2071-2100	Unconstrained	Unconstrained
32	2041-2070	Fire-mediated fuels	Constrained	CanESM2	300 x 10	2011-2040 fire-mediated	2041-2070	Baseline (1981-2010 weather)	Baseline (1980-2010 weather)

ID	Time Period	Fuel Scenario	Fire Regime Scenario	GCM	Iterations	Fuel	Weather	Number of escaped fires	Spread day distribution
33	2071-2100	Fire-mediated fuels	Constrained	CanESM2	300 x 10	2041-2070 fire-mediated	2071-2100	Baseline (1981-2010 weather)	Baseline (1980-2010 weather)
34	2041-2070	Fire-mediated fuels	Constrained	CSIRO	300 x 10	2011-2040 fire-mediated	2041-2070	Baseline (1981-2010 weather)	Baseline (1980-2010 weather)
35	2071-2100	Fire-mediated fuels	Constrained	CSIRO	300 x 10	2041-2070 fire-mediated	2071-2100	Baseline (1981-2010 weather)	Baseline (1980-2010 weather)
36	2041-2070	Fire-mediated fuels	Constrained	HadGEM2	300 x 10	2011-2040 fire-mediated	2041-2070	Baseline (1981-2010 weather)	Baseline (1980-2010 weather)
37	2071-2100	Fire-mediated fuels	Constrained	HadGEM2	300 x 10	2041-2070 fire-mediated	2071-2100	Baseline (1981-2010 weather)	Baseline (1980-2010 weather)
38	2041-2070	Fire-mediated fuels	Unconstrained	CanESM2	300 x 10	2011-2040 fire-mediated	2041-2070	Unconstrained	Unconstrained
39	2071-2100	Fire-mediated fuels	Unconstrained	CanESM2	300 x 10	2041-2070 fire-mediated	2071-2100	Unconstrained	Unconstrained
40	2041-2070	Fire-mediated fuels	Unconstrained	CSIRO	300 x 10	2011-2040 fire-mediated	2041-2070	Unconstrained	Unconstrained
41	2071-2100	Fire-mediated fuels	Unconstrained	CSIRO	300 x 10	2041-2070 fire-mediated	2071-2100	Unconstrained	Unconstrained
42	2041-2070	Fire-mediated fuels	Unconstrained	HadGEM2	300 x 10	2011-2040 fire-mediated	2041-2070	Unconstrained	Unconstrained
43	2071-2100	Fire-mediated fuels	Unconstrained	HadGEM2	300 x 10	2041-2070 fire-mediated	2071-2100	Unconstrained	Unconstrained

Table S2. Coefficients and diagnostics for linear regression models used to predict the future number of escaped fires per year in each fire zone. Temperature = mean noon temperature.

	Great Slave Lake	Southern Prairies	Southern Cordillera
Intercept	-90.3	-54.6	-57.4
β coefficient (July temperature)	6.8	5.7	5.1
β coefficient (August precipitation)	-10.2	-	-
β coefficient (June precipitation)	-	-10.3	-6.5
Adjusted R^2	0.287	0.221	0.508

Table S3. Effects of varying different fire regime components on annual area burned: (a) spread days manipulated; (b) number of fires manipulated; (c) number of fires and spread days manipulated; (d) baseline parameters held constant. Results are for the CSIRO GCM and the 2071-2100 time period.

(a) Spread days manipulated

Mean fire size (ha)	Season		
Zone	Spring	Summer	Grand Total
Great Slave Lake	61,686	18,724	23,685
Southern Cordillera	20,752	24,489	22,498
Southern Prairies	29,988	16,922	23,388
Grand Total	32,998	18,076	23,453
Mean annual number of fires		Season	
Zone	Spring	Summer	Grand Total
Great Slave Lake	2	18	21
Southern Cordillera	1	1	3
Southern Prairies	17	17	34
Grand Total	61,748	109,626	171,374
Annual area burned (ha) =	146,216	339,904	486,120
mean size (ha) *	29,606	30,660	60,266
num fires	503,366	289,987	793,353

(b) Number of fires manipulated

Mean fire size (ha)	Season		
Zone	Spring	Summer	Grand Total
Great Slave Lake	37,143	11,912	14,842
Southern Cordillera	11,370	14,087	12,641
Southern Prairies	9,897	6,207	8,075
Grand Total	12,749	9,070	10,457
Number of fires	Season		
Zone	Spring	Summer	Grand Total
Great Slave Lake	5	42	47
Southern Cordillera	2	2	4
Southern Prairies	46	45	91
Grand Total	160,393	264,849	425,242
Annual area burned =	203,086	496,719	700,022
mean size (ha) *	24,070	26,666	50,691
num fires	454,048	277,397	731,336

(c) Number of fires and spread days manipulated

Mean fire size (ha)	Season		
Zone	Spring	Summer	Grand Total
Great Slave Lake	60,035	20,056	24,581
Southern Cordillera	20,460	24,364	22,350
Southern Prairies	29,444	18,985	23,891
Grand Total	32,119	19,562	24,065
Number of fires	Season		
Zone	Spring	Summer	Grand Total
Great Slave Lake	5	40	45
Southern Cordillera	2	2	4
Southern Prairies	45	47	92
Grand Total	157,266	267,437	424,703
Annual area burned =	308,722	806,512	1,114,892
mean size (ha) *	42,099	45,407	87,640
num fires	1,331,531	893,579	2,204,900

(d) Baseline fire regime

Mean fire size	Season		
Zone	Spring	Summer	Grand Total
2	38,630	11,964	15,109
3	11,150	12,832	11,930
15	9,956	6,241	8,132
Grand Total	13,451	9,414	10,892
Number of fires	Season		
Zone	Spring	Summer	Grand Total
2	3	19	21
3	2	1	3
15	17	17	34
Grand Total	63,736	110,403	174,139
Annual area burned =	97,617	226,144	323,761
mean size (ha) *	16,856	16,763	33,619
num fires	171,307	103,547	274,854

Ecosphere

Wildfire-mediated vegetation change in boreal forests of Alberta, Canada

Diana Stralberg, Xianli Wang, Marc-André Parisien, François-Nicolas Robinne, Péter Solymos, C. Lisa Mahon, Scott E. Nielsen, and Erin M. Bayne

Appendix S3. Modeling and simulation results

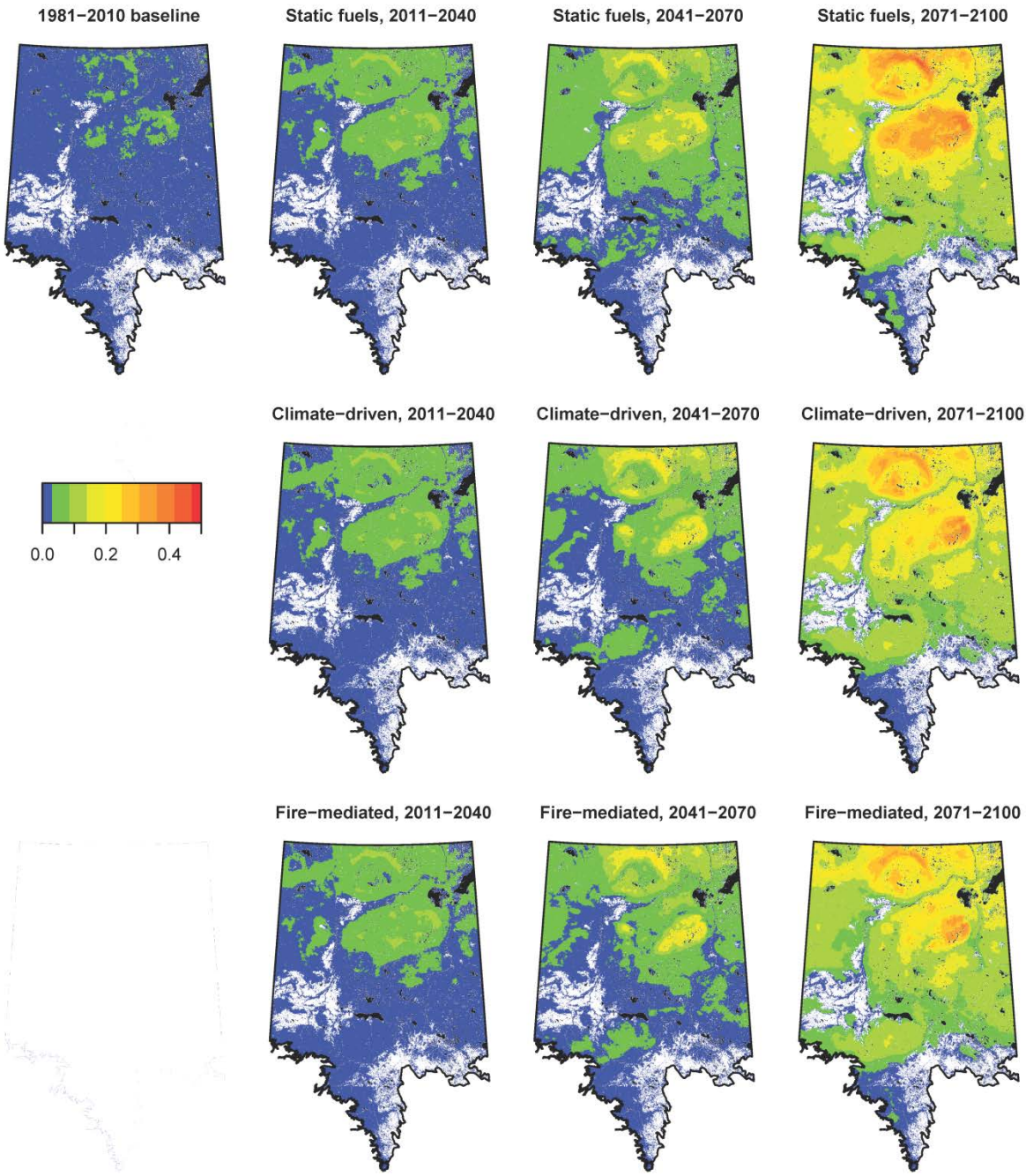

Figure S1. Mean burn probability for each time period and fuel scenario, based on an unconstrained future fire regime. Burn probabilities were averaged across 3000 iterations (10 fuel inputs x 300 runs for fire-mediated scenario). White areas represent non-fuel types.

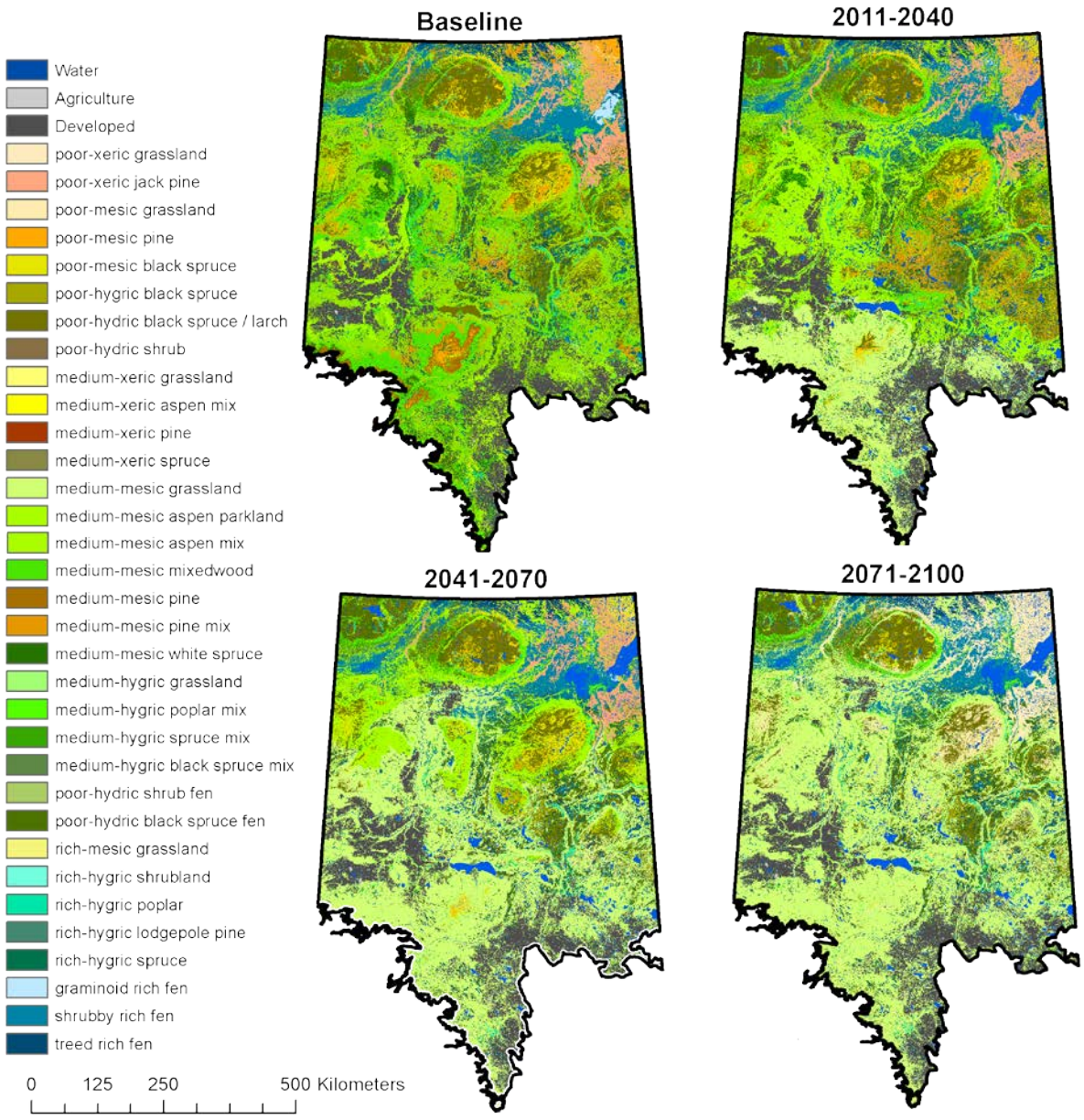

Figure S2. Projected climate-driven vegetation potential for baseline and future time periods, based on the CSIRO global climate model.

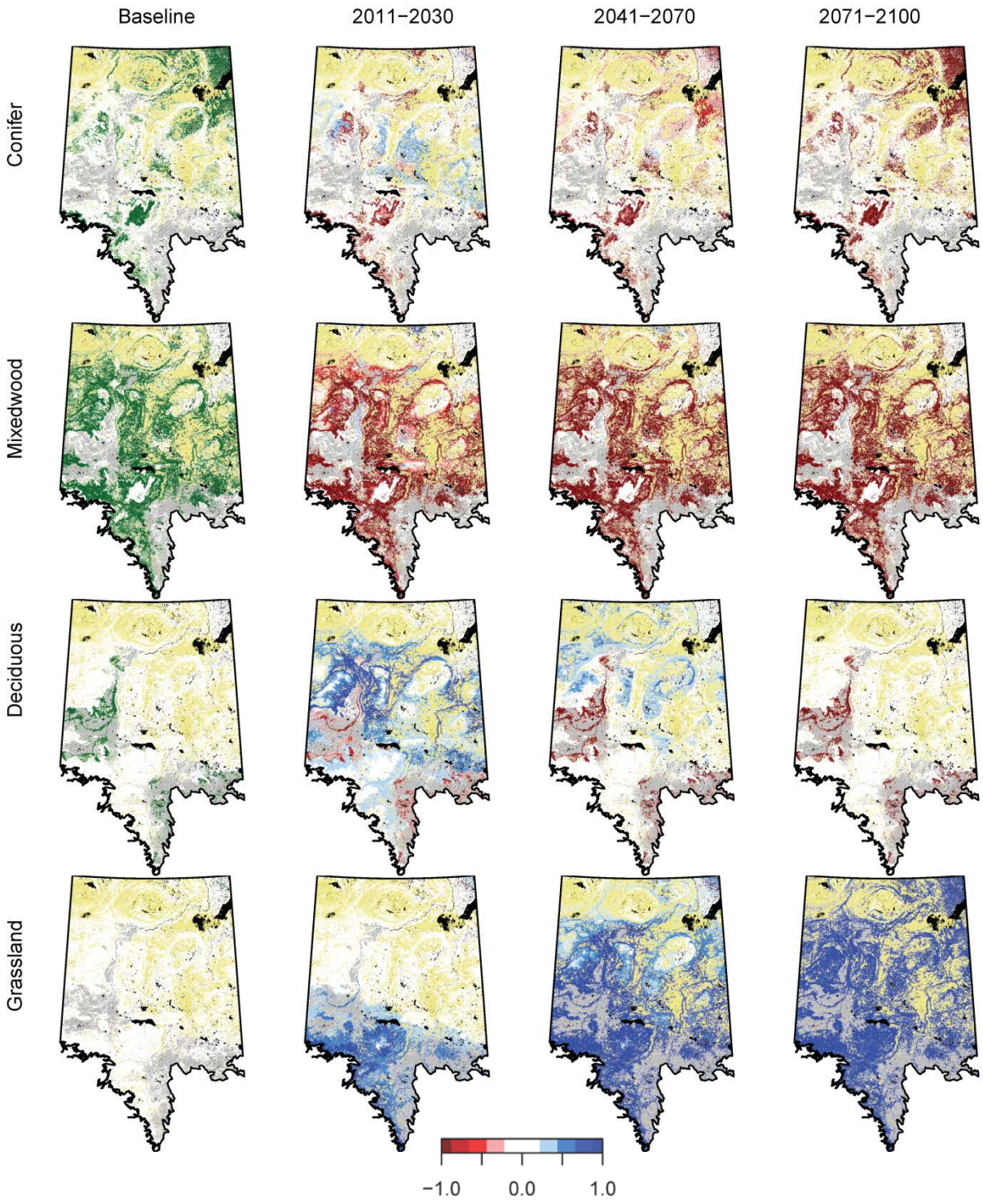

Figure S3. Predicted proportional change in conifer, mixedwood, deciduous, and grassland vegetation types for current and three future time periods under a climate-driven scenario. Proportions based on 3 GCMs. Baseline modelled vegetation shown in green in first column. Black = open water; gray = non-fuel; beige = lowland vegetation.

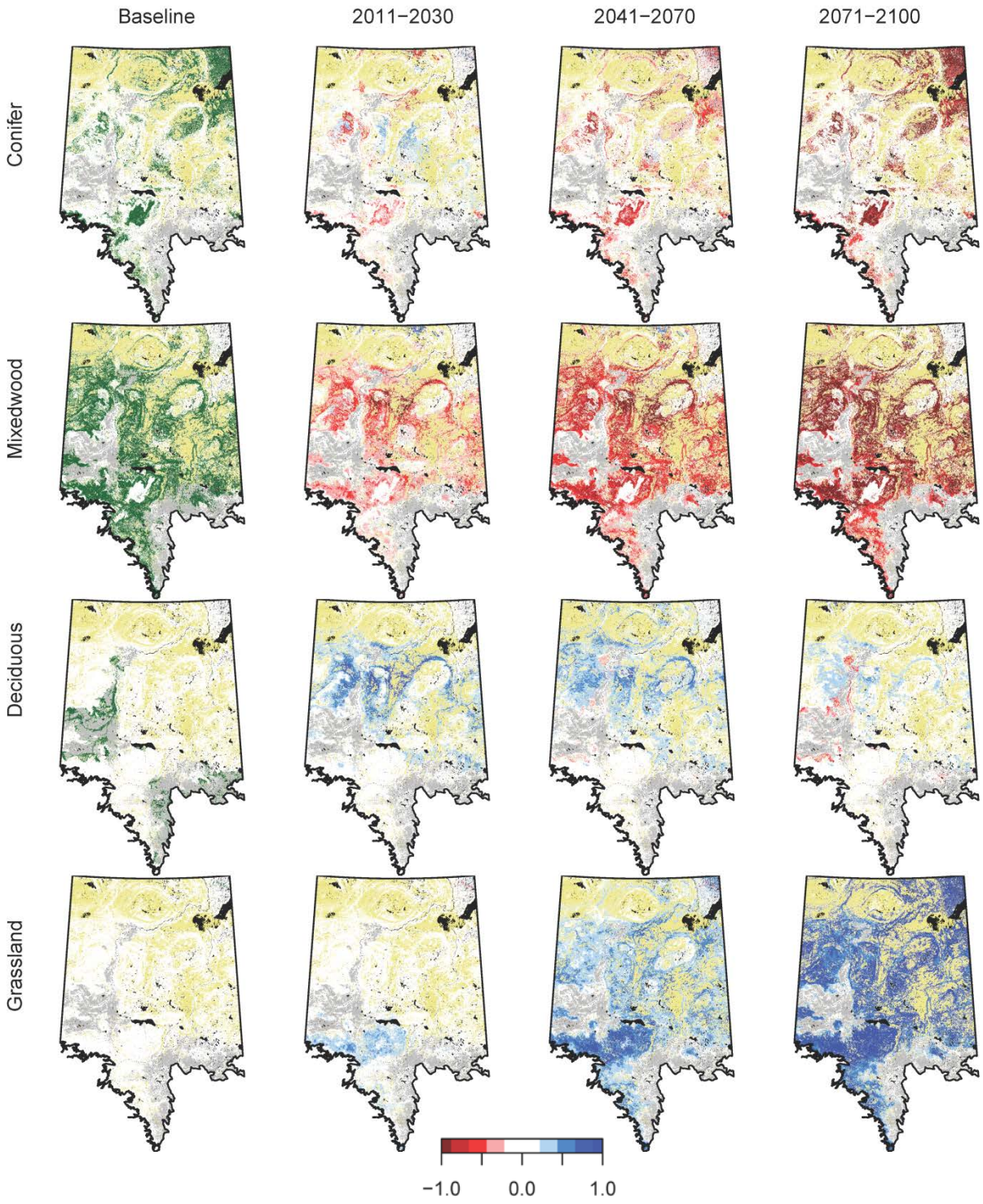

Figure S4. Predicted proportional change in conifer, mixedwood, deciduous, and grassland vegetation types for current and three future time periods under a fire-mediated scenario based on an unconstrained fire regime. Proportions based on 10 fuel realizations x 3 GCMs. Baseline modelled vegetation shown in green in first column. Black = open water; gray = non-fuel; beige = lowland vegetation.

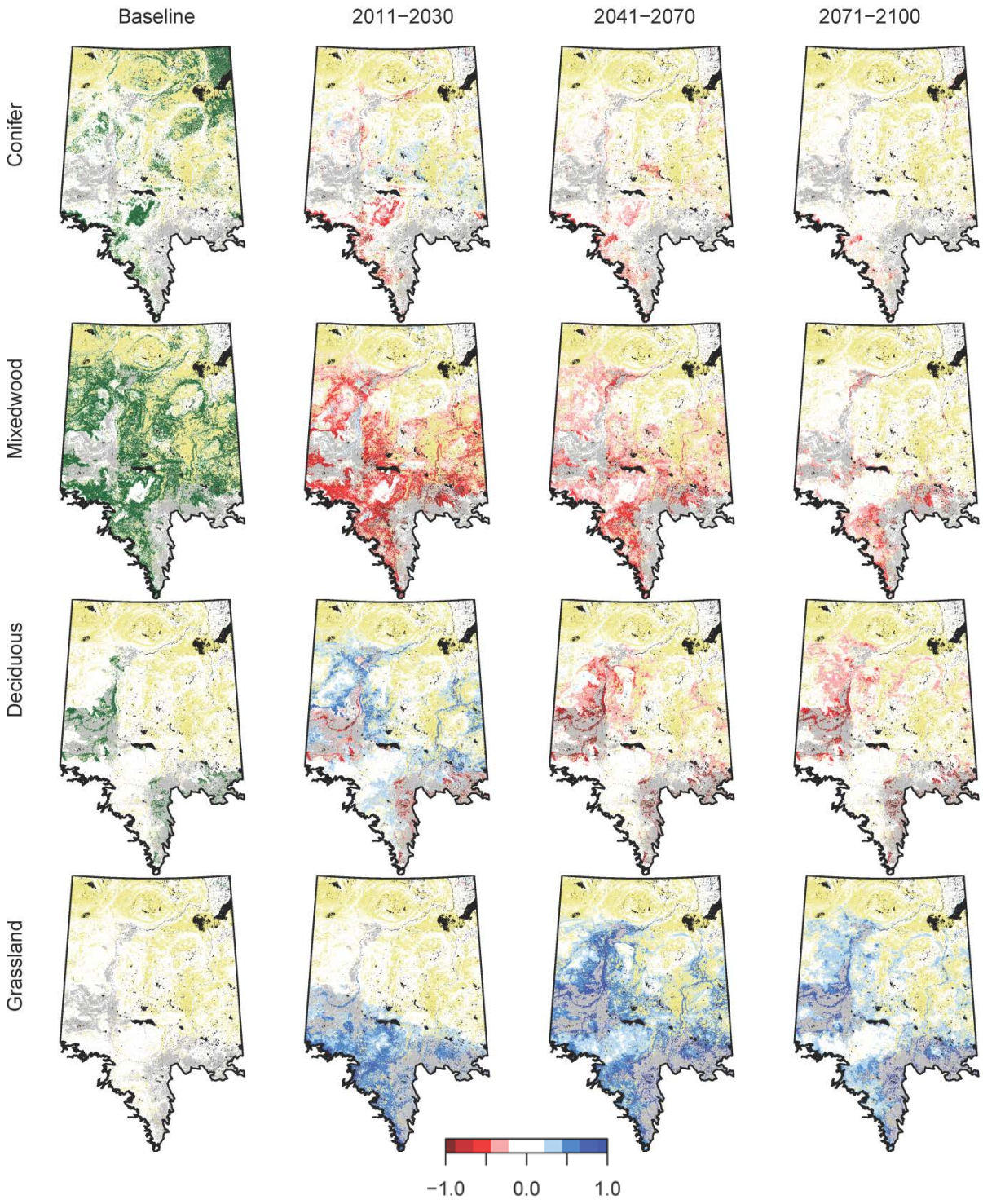

Figure S5. Difference between climate-driven and fire-mediated proportional change in conifer, mixedwood, deciduous, and grassland vegetation types for three future time periods under a fire-mediated scenario based on an unconstrained fire regime. Proportions based on 10 fuel realizations x 3 GCMs. Baseline modelled vegetation shown in green in first column. Black = open water; gray = non-fuel; beige = lowland vegetation.